

Towards Open Vocabulary Learning: A Survey

Jianzong Wu*, Xiangtai Li*, Shilin Xu*, Haobo Yuan*, Henghui Ding, Yibo Yang, Xia Li, Jiangning Zhang, Yunhai Tong, Xudong Jiang, Bernard Ghanem, Dacheng Tao

Abstract—In the field of visual scene understanding, deep neural networks have made impressive advancements in various core tasks like segmentation, tracking, and detection. However, most approaches operate on the close-set assumption, meaning that the model can only identify pre-defined categories that are present in the training set. Recently, open vocabulary settings were proposed due to the rapid progress of vision language pre-training. These new approaches seek to locate and recognize categories beyond the annotated label space. The open vocabulary approach is more general, practical, and effective than weakly supervised and zero-shot settings. This paper thoroughly reviews open vocabulary learning, summarizing and analyzing recent developments in the field. In particular, we begin by juxtaposing open vocabulary learning with analogous concepts such as zero-shot learning, open-set recognition, and out-of-distribution detection. Subsequently, we examine several pertinent tasks within the realms of segmentation and detection, encompassing long-tail problems, few-shot, and zero-shot settings. As a foundation for our method survey, we first elucidate the fundamental principles of detection and segmentation in close-set scenarios. Next, we examine various contexts where open vocabulary learning is employed, pinpointing recurring design elements and central themes. This is followed by a comparative analysis of recent detection and segmentation methodologies in commonly used datasets and benchmarks. Our review culminates with a synthesis of insights, challenges, and discourse on prospective research trajectories. To our knowledge, this constitutes the inaugural exhaustive literature review on open vocabulary learning. We keep tracing related works at <https://github.com/jianzongwu/Awesome-Open-Vocabulary>.

Index Terms—Open Vocabulary, Scene Understanding, Object Detection, Segmentation, Survey

1 INTRODUCTION

DEEP neural networks have revolutionized scene understanding tasks, including object detection, segmentation, and tracking [1], [2], [3], [4]. Nonetheless, using conventional approaches for real-world applications can be challenging due to limitations such as inadequate class annotations, close-set class definitions, and costly labeling expenses. These limitations can increase the difficulty and cost of implementing a deep model on new scenes, particularly when the number of categories or concepts in the scene is much larger than what is included in the training dataset.

For example, object detection is a core task in computer vision that involves scene understanding. It requires human annotations for each category and each object location, which can be costly and time-consuming. For instance, the COCO dataset [5], which is widely used for benchmarking object detection algorithms, only includes 80 categories. But in reality, natural scene images often have more than 80 different types of objects. To extend object detectors to cover all these categories, we would need to

incur significant annotation costs. Current research focuses on developing methods to train more flexible object detectors on the subset of COCO with base classes and let them identify new or unfamiliar objects without requiring additional annotations.

Several previous solutions are to adopt zero-shot learning (ZSL) [6], [7], [8]. These approaches extend a detector to generalize from annotated (seen) object classes to other (unseen) categories. The annotations of seen object classes are used during the training, while the annotations of unseen classes are *strictly* unavailable during training. Most approaches adopt word embedding projection to constitute the classifier for unseen class classification.

However, these approaches come with several limitations. ZSL, in particular, is highly restrictive. Typically, these methods lack examples of unseen objects and treat these objects as background objects during training. As a result, during inference, the model identifies novel classes solely based on their pre-defined word embeddings [9], [10], [11], thereby limiting exploration of the visual information and relationships of those unseen classes. This is why ZSL approaches have been shown to yield unsatisfying results in novel classes.

Open vocabulary learning is proposed to handle the above issue and make the detector extendable. It has been successfully applied to multiple tasks, e.g., segmentation, detection, video understanding, scene understanding, etc. In particular, open vocabulary object detection [12], [13] is first proposed. Also, open vocabulary segmentation is proposed [14], [15]. Similarly, the model trains on base classes and inferences on both base and novel classes. The critical difference between zero-shot learning and open vocabulary is that one can use *visual-related language vocabulary data* like image captions as auxiliary supervision in

• J. Wu, S. Xu, X. Li, and Y. Tong are with the National Key Laboratory of General Artificial Intelligence, School of Intelligence Science and Technology, Peking University, Beijing, China.
 • H. Ding, X. Jiang are with Nanyang Technological University, Singapore.
 • H. Yuan is with Wuhan University, Wuhan, China.
 • Y. Yang and B. Ghanem are with King Abdullah University of Science and Technology, Saudi Arabia.
 • D. Tao is with the University of Sydney, Sydney, Australia.
 • X. Li is with ETH Zurich, Switzerland.
 • J. Zhang is with Zhejiang University, Hangzhou, China.
 • The *first four authors* share the same contribution to this work. Email: jzwu@stu.pku.edu.cn, lxtpk@pku.edu.cn, xushilin@stu.pku.edu.cn.

open vocabulary settings. The motivations to use language data as auxiliary weak supervision are: 1) Language data requires less labeling effort and thus is more cost-friendly. The visual-related language data, like image captions, is widely available and more affordable than box or mask annotations. 2) Language data provides a more extensive vocabulary size and thus is more extendable and general. For example, words in captions are not limited to the pre-defined base categories. It may contain novel class names, attributes, and motions of objects. Incorporating captions in training is proved to be extremely useful in helping improve the models' scalability.

Moreover, recently, visual language models (VLMs) [16], [17], which pre-train themselves on large-scale image-text pairs, show remarkable zero-shot performance on various vision tasks. The VLMs align images and language vocabularies into the same feature space, fulfilling the gap between visual and language data. Many open vocabulary methods effectively eliminate the distinction between close-set and open-set scenarios by utilizing the alignment learned in VLMs, making them highly suitable for practical applications. For example, An open vocabulary object detector can be easily extended to other domains according to the demand without the need to gather relevant data or incur additional labeling expenses.

As open vocabulary models continue to advance rapidly and demonstrate impressive results, it is worthwhile to track and compare recent research on open vocabulary learning. Several surveys work on low-shot learning [18], [19], [20], [21], including few-shot learning and zero-shot learning. There are also several surveys on multi-modal learning [22], [23], including using transformer for vision language tasks [22], [24] and vision language pre-training [25]. However, these works focus on learning with few examples, multi-modal fusion, or pre-training for better feature representation. As far as we know, there haven't been any surveys that thoroughly summarize the latest developments in open vocabulary learning, including methods, settings, benchmarks, and the use of vision foundation models. We aim to fulfill the blank with this work.

Contribution. In this survey, we systematically track and summarize recent literature on open vocabulary learning, including object detection, segmentation, video understanding, and 3D scene understanding. The survey covers the most representative works in each domain by extracting the common technical details. It also contains the background of open vocabulary learning and related concepts comparison, including zero-shot learning (ZSL) [26], open set recognition (OSR) [27], [28], and out-of-distribution detection (OOD) [29]. It also includes large-scale visual language models and representative detection and segmentation works, which makes the survey self-contained. In addition, we present a comprehensive analysis and comparison of benchmarks and settings for each specific domain. As far as we know, we are the first to concentrate on the specific area. Finally, since the field of open vocabulary learning is rapidly evolving, we may not be able to keep up with all the latest developments. We welcome researchers to contact us and share their new findings in this area to keep us updated. Those new works will be included and discussed in the revised version.

Survey pipeline. In Sec. 2, we will cover the background knowledge, including definition, datasets, metrics, and related research domains. Then, in Sec. 3, we conduct main reviews on various methods according to different tasks. In particular, we will first include the preliminary knowledge of close-set detection and

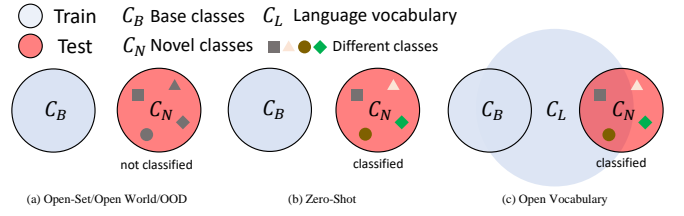


Fig. 1: Concepts comparison between open-set/open world/out-of-distribution detection (OOD), zero-shot and open vocabulary. Different shapes represent different novel categories. Colors represent the predictions of the novel objects. (a), in the open-set/Open World/OOD settings, the model only needs to identify novel classes and mark them as 'unknown.' (b) in the zero-shot setting, a model must classify novel classes into specific categories. (c) in the open vocabulary settings, the model can classify novel classes with the help of large language vocabulary knowledge C_L .

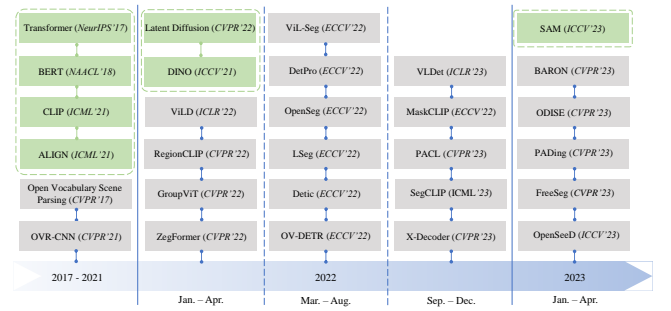


Fig. 2: Timeline of open vocabulary learning. The gray boxes indicate representative works. Green boxes indicate the foundation models and VLMs. In open vocabulary learning, many works exploit the knowledge learned by pre-trained vision foundation models like Swin [30] and VLMs like CLIP [16]. Recently, some works also explore the use of diffusion models in this setting.

segmentation methods. Then we present the method details of each direction, including detection, segmentation, video understanding, and 3D scene understanding. In Sec. 4, we compare the results for different tasks and benchmarks. We point out future directions in Sec. 5 and draw conclusions at Sec. 6.

2 BACKGROUND

Overview. In this section, we first present the concept definition of open vocabulary and related concepts comparison. Then, we present a historical review of open vocabulary learning and point out several representatives. Next, we present the standard datasets and metrics. We also present the unified notations for open vocabulary object detection and segmentation tasks. Finally, we review the related research domains.

2.1 Concept Definition

Taking the classification task as an example, the traditional supervised methods assume that the training data and testing data share the same closed-set label space. However, the model trained under this assumption cannot be extended to new or different categories. To address this issue, researchers have introduced concepts like

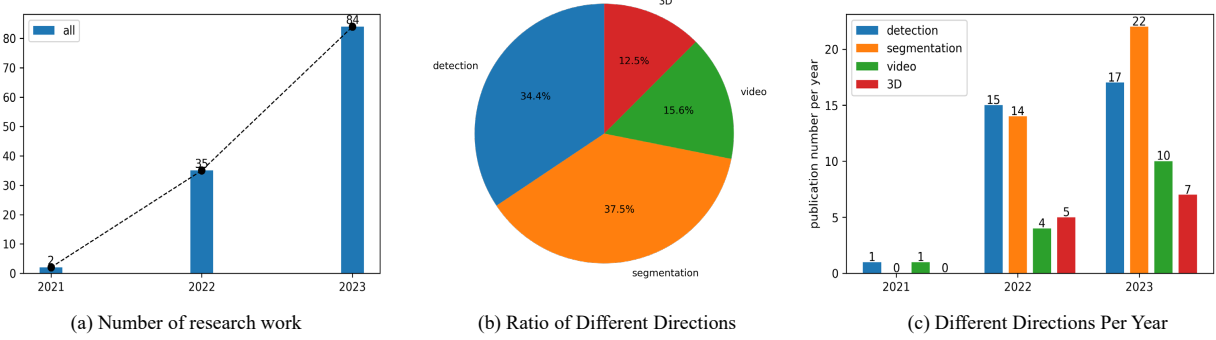


Fig. 3: Summarization on open vocabulary learning research works. (a), The number of research works still increases. (b) Both detection and segmentation have larger numbers than 3D and video. (c) indicates each direction per year. The results are obtained on 2023/7/20.

open-set learning and zero-shot learning, ultimately leading to open vocabulary learning.

We first compare these closely related concepts in Fig. 1, including open-set, open world, OOD, zero-shot learning, and open vocabulary learning. These concepts have similar settings and notations. In particular, the examples are classified into base and novel classes (or out-of-distribution examples). The base classes are used for training, while the novel classes are not. We denote the base classes in the label set space C_B and the novel classes in the label set space C_N .

The open-set, open world, and OOD tasks share the same testing procedure. Models only need to identify novel categories and set them as one label, named 'unknown.' Models do not need to identify the specific class categories in such settings. The process is shown in Fig. 1(a). Then, on the contrary, zero-shot learning goes beyond these three settings by further categorizing the novel objects, as shown in Fig. 1 (b). From such a perspective, zero-shot learning is a more challenging setting.

Due to the lower performance on novel classes in practice and the easier acquisition of image-text pairs, recent works [12], [13] propose the open vocabulary settings. It allows using additional low-cost training data or pre-trained vision language models like CLIP, which have much larger language vocabularies C_L . C_L may contain the concepts of both C_B and C_N , which enables model to generalize across novel classes. We summarize the concept's differences as follows:

- **Open-Set/Open World/OOD.** The three tasks only demand the model to identify and reject unknown objects from the classification. The model only needs to find unknown classes or examples without classifying them into different classes.

- **Zero-Shot Learning.** The model has strictly trained on C_B class examples where the C_N is unavailable during training. The model needs to predict the specific categories for novel objects.

- **Open Vocabulary Learning.** Based on the zero-shot learning setting, one can acquire an additional low-cost training source or knowledge C_L , large-scale language vocabulary. For example, image captions are the most commonly used language data to help extend the semantic space of an open vocabulary model. One can also use the pre-trained vision language models by adapting them for novel class classification. Note that C_L is not strictly required to contain C_B or C_N , as the language vocabulary may not cover all the class names in the vision data. On the contrary, C_L may also have words out of the pre-defined novel categories, which can further extend models' generalizability.

2.2 History and Roadmap

Before introducing the open vocabulary setting, reviewing the progress of open vocabulary learning is necessary. In Fig. 2, we summarize the timeline of open vocabulary learning. Localization and classification of arbitrary objects in the wild have been challenging problems due to the limitations of existing datasets. The concept of open vocabulary in scene understanding comes from the work [31], where the authors build a joint image pixel and word concept embedding framework. The concept is hierarchically divided. Then, multi-modal pre-training was well studied with the rise of BERT [9] in NLP. Motivated by the process of vision language pre-training, OVR-CNN [12] proposed the concept of open vocabulary object detection, where the caption data are used for connecting novel classes semantics and visual region. Later on, CLIP was presented and open-sourced. After that, ViLD [13] is the first work that uses the knowledge of CLIP to build open vocabulary object detection. Meanwhile, LSeg [15] first explored the CLIP knowledge of language-driven segmentation tasks. After these works, recently, there have been more and more works on improving the performance of open vocabulary detectors or building new benchmarks for various settings. Recently, PADing [32] explored the unified open vocabulary learning framework for three different segmentation tasks. SAM [33] is proposed to build the segmentation foundation model, which is trained by billion-level masks. Combined with CLIP, SAM can also achieve good zero-shot segmentation without fine-tuning. Recently, with the rapid process of large language model (LLM) [34], open vocabulary learning has become a more promising direction since more language knowledge can be embedded in multi-modal architecture. As shown in Fig. 3(a), the number of research works in open vocabulary learning has increased significantly since 2021. We also summarize the statistics of different directions in Fig. 3(b) and (c). The details of these directions can be found in Sec. 3.

2.3 Tasks, DataSets, and Metrics

- **Tasks.** Open vocabulary learning has included a wide range of computer vision tasks, including object detection [12], [35], [36], segmentation [37], [38], [39], video understanding, and 3D scene understanding. The center goal of these tasks is similar, recognizing the novel classes with the aid of large vocabulary knowledge for their corresponding tasks. In this survey, we mainly focus on the methods of scene understanding tasks, including object detection, instance segmentation, semantic segmentation, and object tracking. Nonetheless, we also consider other closely

related tasks, such as open vocabulary attribution prediction, video classification, and point cloud classification.

- **Dataset.** For object detection, the common datasets are COCO [5] and LVIS [40]. Recently, a more challenging dataset, v3Det [41] with more than 10,000 categories, is proposed. For image segmentation, the most commonly used datasets are COCO [5], ADE20k [42], PASCAL-VOC 2012 [43], PASCAL-Context [44], and Cityscapes [45]. For video segmentation and tracking, the frequently used datasets are VSPW [46], YouTube-VIS [47], LV-VIS [48], MOSE [49], and TAO [50].

- **Metrics.** For detection tasks, the commonly used metrics are mean average precision (mAP) and mean average recall (mAP) for both base classes and novel classes. As for segmentation tasks, the commonly used metrics are mean intersection over union (mIoU) for semantic segmentation, mask-based mAP for instance segmentation, and panoptic quality (PQ) for panoptic segmentation.

2.4 Related Research Domains

- **Long-tail Object Detection and Instance Segmentation.** This task addresses the challenge of class imbalance in instance segmentation. Many approaches tackle this issue through techniques such as data re-sampling [40], [51], [52], loss re-weighting [53], [54], [55], and decoupled training [56], [57]. Specifically, some studies [51] employ image-level re-sampling. However, these methods tend to introduce bias in instance co-occurrence. To address this issue, other works [52], [58], [59] focus on more refined re-sampling techniques at the instance or feature level. Regarding loss re-weighting, most studies [53], [54] rebalance the ratio of positive and negative samples during training. Additionally, decoupled training methods [56], [57] introduce different calibration frameworks to enhance classification results. Resolving long-tail object detection can lead to improved accuracy in detecting novel classes. However, the proposed methods currently cannot be applied to the detection of novel classes.

- **Few-Shot Detection and Segmentation:** Few-shot object detection aims to expand the detection capabilities of a model using only a few labeled samples. Several approaches [60], [61], [62], [63], [64], [65], [66], [67], [68] have been proposed to advance this field. Notably, TFA [69] introduces a simple two-phase fine-tuning method, while DeFRCN [70] separates the training of RPN features and RoI classification. Moreover, SRR-FSD [71] combines multi-modal inputs while LVC [72] proposes a pipeline to generate additional examples for novel object detection and train a more robust detector. Few-shot segmentation comprises Few-Shot Semantic Segmentation (FSSS) and Few-Shot Instance Segmentation (FSIS). FSSS involves performing pixel-level classification on query images. Previous approaches [73], [74], [75], [76], [77], [78], [79] typically build category prototypes from support images and segment the query image by computing the similarity distance between each prototype and query features. On the other hand, FSIS aims to detect and segment objects with only a few examples. FSIS methods can be categorized into single-branch and dual-branch methods. The former [80], [81] primarily focuses on designing the classification head, while the latter [82], [83], [84] introduce an additional support branch to compute class prototypes or re-weighting vectors of support images. This support branch assists the segmenter in identifying target category features through feature aggregation. For example, Meta R-CNN [84] performs channel-wise multiplication on RoI

features, and FGN [83] aggregates channel-wise features at three stages: RPN, detection head, and mask head. However, few-shot learning methods still require examples of novel classes during training, and such data or annotations may not be available.

- **Zero-Shot Detection and Segmentation:** This task aims to segment classes that have not been encountered during training. Two streams of work have emerged: discriminative methods [85], [86], [87], [88], [89] and generative methods [90], [91], [92]. Representative works in this field include SPNet [85] and ZS3Net [90]. SPNet [85] maps each pixel to a semantic word embedding space and projects pixel features onto class probabilities using a fixed semantic word embedding [93], [94] projection matrix. On the other hand, ZS3Net [90] first trains a generative model to produce pixel-wise features for unseen classes based on word embeddings. With these synthetic features, the model can be trained in a supervised manner. Both of these works treat zero-shot detection and segmentation as a pixel-level zero-shot classification problem. However, this formulation is not robust for zero-shot learning, as text embeddings are typically used to describe objects/segments rather than individual pixels. Subsequent works [32], [91], [92], [95], [96], [97] follow this formulation to address different challenges in zero-shot learning. In a weaker assumption where unlabeled pixels from unseen classes are available in the training images, self-training [87], [90] is commonly employed. Despite promising results, self-training often requires model retraining whenever a new class appears. ZSI [98] also employs region-level classification for bounding boxes but focuses on instance segmentation rather than semantic segmentation. More recently, PADing [32] proposes a unified framework to tackle zero-shot semantic segmentation, zero-shot instance segmentation, and zero-shot panoptic segmentation.

Most approaches in open vocabulary learning are based on zero-shot learning settings, such as replacing the fixed classifier with language embeddings. However, these methods struggle to generalize well to novel classes due to the absence of novel class knowledge. Consequently, their performance is limited, and they are not practical for real-world applications.

3 METHODS: A SURVEY

Overview. In this section, we first review several basic concepts and network architecture as preliminary knowledge by extending close-set detectors into open vocabulary detectors. Then we sequentially survey the six subsidiary tasks, including object detection (Sec. 3.2), segmentation (Sec. 3.3), video understanding (Sec. 3.4), 3D scene understanding (Sec. 3.5), and closely related tasks (Sec. 3.6). Note that we only record and compare the most representative works. We list numerous works in Tab. 1 and Tab. 4. Moreover, since there are several similar tasks (Sec. 3.6), we also survey and compare other related tasks, including class agnostic detection and segmentation, open world object detection, and open-set panoptic segmentation.

3.1 Preliminary

Pixel-based Object Detection and Segmentation. In general, it can be divided into two aspects: *semantic-level* tasks and *instance-level* tasks, where the difference lies in whether to distinguish each instance. For the former, we take semantic segmentation as an example. It was typically approached as a dense pixel classification problem, as initially proposed by FCN [99]. Then, the following works are all based on the FCN framework [100]. These methods

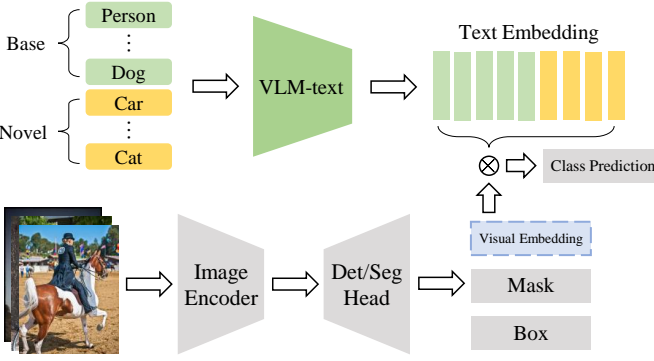


Fig. 4: An illustration of a common architecture in open vocabulary object detection and segmentation. The vision model predicts a class embedding for each box/mask. The embeddings are compared to a set of class embeddings generated by a VLM text model like CLIP or ALIGN, using dot products. The class with the highest score is chosen as the predicted label for the object. Note that while humans define the set of possible object classes, the system only has access to a limited set of "base" classes during training.

can be divided into the following categories, including better encoder-decoder frameworks [101], [102], larger kernels [103], multiscale pooling [104], [105], multiscale feature fusion [106], [107], [108], [109], non-local modeling [110], and better boundary delineation [111], [112], [113], [114]. After the transformer was proposed, with the goal of global context modeling, several works propose the variants of self-attention operators to replace the CNN prediction heads [115], [116].

For the latter, we take object detection and instance segmentation for illustration. Object detection aims to detect each instance box and classify each instance. It mainly has two different categories: two-stage approaches and one-stage approaches. Two-stage approaches [2], [117] rely on an extra region proposal network (RPN) to recall foreground objects at the first stage. Then, the proposals (Region of Interests, RoI) with high scores are sent to the second-stage detection heads for further refinement. One-stage approaches [118], [119] directly output each box and label in a per-pixel manner. In particular, with the help of focal loss and feature pyramid networks, one-stage approaches can surpass the two-stage methods in several datasets. Both approaches need anchors for the regression of the bounding box. The anchors are the pixel locations where the objects are possibly emerging. Since two-stage approaches explicitly explore the foreground objects, where they have better recall than single-stage approaches. Two-stage approaches are more commonly used in open vocabulary object detection tasks.

Instance segmentation segmenting each object goes beyond object detection. Most instance segmentation approaches focus on how to represent instance masks beyond object detection, which can be divided into two categories: top-down approaches [2], [120] and bottom-up approaches [121], [122]. The former extends the object detector with an extra mask head. The designs of mask heads are various, including FCN heads [2], [123], diverse mask encodings [124], and dynamic kernels [120], [125]. The latter performs instance clustering from semantic segmentation maps to form instance masks. The performance of top-down approaches is

closely related to the choice of detectors [126], while bottom-up approaches depend on both semantic segmentation results and clustering methods [127]. Besides, there are also several approaches [128] using grid representation to learn instance masks directly.

Query-based Object Detection and Segmentation. With the rise of vision transformers [3], [4], recent works mainly use transformer-based approaches in segmentation, detection, and video understanding. Compared with previous pixel-based approaches, transformer-based approaches have more advantages in cases of flexibility, simplicity, and uniformity [4], [49], [129], [130], [131], [132], [133], [134], [135], [136], [137]. One representative work is detection transformer (DETR) [4]. It contains a CNN backbone, a standard transformer encoder, and a standard transformer decoder. It also introduces the concepts of object query to replace the anchor design in pixel-based approaches. Object query is usually combined with bipartite matching [138] during training, uniquely assigning predictions with ground truth. This means each object query builds the one-to-one matching during training. Such matching is based on the matching cost between ground truth and predictions. The matching cost is defined as the distance between prediction and ground truth, including labels, boxes, and masks. By minimizing the cost with the Hungarian algorithm [138], each object query is assigned by its corresponding ground truth. For object detection, each object query is trained with classification and box regression loss [117]. For instance-wised segmentation, each object query is trained with classification loss and segmentation loss. The output masks are obtained via the inner product between object query and decoder features. Recently, mask transformers [139], [140], [141] further removed the box head for segmentation tasks. Max-Deeplab [139] is the first to remove the box head and design a pure-mask-based segmenter. It combines a CNN-transformer hybrid encoder [142] and a query-based decoder as an extra path. Max-Deeplab still needs many auxiliary loss functions. Later, K-Net [140] uses mask pooling to group the mask features and designs a dynamic convolution to update the corresponding query. Meanwhile, MaskFormer [141] extends the original DETR by removing the box head and transferring the object query into the mask query via MLPs. It proves simple mask classification can work well enough for all three segmentation tasks. Then, Mask2Former [143] proposes masked cross-attention and replaces the cross-attention in MaskFormer. Masked cross-attention forces the object query only attends to the object area, guided by the mask outputs from previous stages. Mask2Former also adopts a stronger Deformable FPN backbone [144], stronger data augmentation [145], and multiscale mask decoding. In summary, query-based approaches are stronger and simpler. They cannot directly detect novel classes but are widely used as base detectors and segmenters in open vocabulary settings.

Large Scale Visual Language Pre-training. Better visual language pre-training can lead to a better understanding of semantics on given visual inputs [130], [131], [146]. Previous works [147], [148], [149] focus on cross-modality research via learning the visual and sentence-dense connection between different modalities. Some works [149], [150] utilize two-stream neural networks based on the vision transformer model, while several works [151], [152] adopt the single-stream neural network, where the text embeddings are frozen. The two-stream neural networks process visual and language information and fuse them afterward by another transformer module. Recently, most approaches [16], [17] adopt pure

transformer-based visual language pre-training. Both CLIP [16] and Align [17] are concurrent works that explore extremely large-scale pre-training on image text pairs. In particular, with such large-scale training, CLIP demonstrates that the simple pre-training task of predicting which caption goes with which image can already lead to stronger generalizable models. These VLMs are the foundation of open vocabulary learning in different tasks, which means that the open vocabulary approaches aim to distill or utilize knowledge of VLMs into their corresponding tasks.

Turning Close-set Detector and Segmente into Open Vocabulary Setting. A common way towards the open vocabulary setting is to replace the fixed classifier weights with the text embeddings from a VLM model. In Fig. 4, we present a meta-architecture. In particular, the vision model generates a visual embedding for each box/mask proposal and computes similarity scores by computing a dot product with the text embeddings from both base and novel classes. The classification scores are computed as follows:

$$p_{ij} = \frac{\exp \langle e_i^v, e_j^t \rangle}{1 + \sum_{j'=1}^{|C_B \cup C_N|} \exp \langle e_i^v, e_{j'}^t \rangle}, \quad (1)$$

where e_i^v is the i -th vision embedding and e_j^t is the j -th text embedding, and p_{ij} is the prediction score of the i -th vision proposal predicted to the j -th class. The $\langle \cdot, \cdot \rangle$ represents the dot product operation. The denominator is added with one because the background text embedding is set to all 0 or make it learnable. C_B and C_N are base and novel classes, respectively. Finally, the class with the highest prediction score is chosen as the prediction. In practice, the vision embeddings are trained with base annotations to fit the text embeddings. Therefore, the model combines the knowledge of VLM and the learned visual features, and the detector/segmente can detect/segment novel classes via semantically related text embeddings.

3.2 Open Vocabulary Object Detection

In this section, we review the approaches for open vocabulary object detection. We divide the methods into five categories: knowledge distillation, region text pre-training, training with more balanced data, prompting modeling, and region text alignment. Finally, we summarize the common features in Tab. 2.

Knowledge Distillation. These techniques aim to distill the knowledge of Vision-and-Language Models (VLMs) into close-set detectors [2], [4], [117]. Since the knowledge of VLMs is much larger than close-set detectors, distilling novel classes into based classes trained detectors is a straightforward idea. One earlier method is ViLD [13], a two-stage detection approach that utilizes instance-level visual-to-visual knowledge distillation. ViLD consists of two branches: the ViLD-text branch and the ViLD-image branch. In the former branch, fixed text embeddings are obtained from VLMs' text encoder output. Meanwhile, in the latter branch, pre-computed proposals are fed into a detector to obtain region embeddings. The cropped image is then sent to the VLMs' image encoder to generate image embeddings. Subsequently, ViLD proposes distilling this information onto each Region-of-Interest (RoI) via \mathcal{L}_1 Loss. HierKD [153] uses a single-stage detector and introduces a global-level language-to-visual knowledge distillation module. The module aims to narrow down performance gaps between one-stage and two-stage methods. This technique employs global-level knowledge distillation modules (GKD), which align global-level image representations

with caption embeddings through contrastive loss. Both ViLD and HierKD use pixel-based detectors. However, Rasheed et al. [177] leverages query-based detector Deformable DETR [144] for its detection process. To ensure consistency between their detection region representations and CLIP's region representations, the authors employed inter-embedding relationship matching loss (IRM). Furthermore, the authors adopt mixed datasets pre-training to enhance the ability of novel class discovery. OADP [178] thinks previous works only distill object-level information from VLMs to downstream detectors and ignore the relation between different objects. To tackle this problem, OADP employs object-level distillation as well as global and block distillation methods. These supplementary techniques aim to compensate for the lack of relational information in object distillation by optimizing the L1 distance between CLIP visual encoder and the detector backbone's global features or block features. Rather than using simple novel class names for text distillation, several works also utilize more fine-grained information, including attributes, captions, and relationships of objects. PCL [179] adopts an image captioning model to generate captions that describe object instances in a more comprehensive way. OVRNet [180] simultaneously detects objects and their visual attributes in open vocabulary scenarios. By exploring COCO attributes dataset [181] via a joint co-training strategy, the authors find that the recognition of fine-grained attributes works complementary for OVD.

Region Text Pre-training. Another assumption of open vocabulary learning is the availability of large-scale image text pairs, which can be easily obtained in daily life. Since these pairs contain large enough knowledge to cover the most novel or unseen datasets for detection and segmentation. The learning of region text alignment maps the novel classes of visual features and text features into an aligned feature space. OVR-CNN [12] first introduces the concept of open vocabulary object detection by using caption data for novel class detection. The model first trains a ResNet [1] and vision to language (V2L) layer using image-caption pairs via grounding, masked language modeling, and image-text matching. Since captions are not constrained in language space, the V2L layer learns to map features from visual space into semantic space without limiting to closed-label space. During the next stage of training, Faster R-CNN [117] is used as a detection method with pre-trained ResNet as its backbone. OVR-CNN [12] replaces only learnable classifiers with fixed text embeddings from pre-trained language models [9]. For classification purposes, region visual features obtained from ROI-Align [2] are sent into the V2L layer and mapped into semantic space. Attribute-Sensitive OVR-CNN [182] proposes a different approach from OVR-CNN [12]. Instead of grounding vision regions to the input word embeddings of BERT [9], Attribute-Sensitive OVR-CNN aligns vision regions with contextualized word embeddings that are output from BERT [9]. Additionally, Attribute-Sensitive OVR-CNN proposes using an adjective-noun negative caption sampling strategy to enhance the model's sensitivity to adjectives, verb phrases, and prepositional phrases other than object nouns in the caption. GLIP series [183], [184] unify the object detection and phrase grounding for pre-training. In particular, it leverages massive image-text pairs by generating grounding boxes in a self-training fashion, which sets strong results for both detection and grounding. RegionCLIP [155] learns visual region representation by matching image regions to region-level descriptions. It creates pseudo labels by CLIP for region-text pairs and then uses contrastive loss to match them before fine-tuning the visual en-

TABLE 1: Representative works summarization and comparison in Sec. 3.2 and Sec. 3.3. We list the training data, detectors or segmenters, VLMs, and highlighted features for comparison.

Method	Task	Text Training Data	Vision Training Annotations	Text Model	Vision Model	Highlight
Open Vocabulary Detection (Sec. 3.2)						
OVR-CNN [12]	OVOD	Captions	Bounding Boxes (Base)	BERT	Faster R-CNN	The first method that proposes OVOD and adopts grounded caption pre-training.
ViLD [13]	OVOD	None	Bounding Boxes (Base)	CLIP-text	CLIP-vision + Faster R-CNN	The first method that distills knowledge from the pre-trained CLIP model.
HierKD [153]	OVOD	None	Bounding Boxes (Base)	CLIP-text	CLIP-vision + ATSS	Distills Global-level knowledge from the pre-trained CLIP model into the one-stage detector.
VL-PLM [154]	OVOD	None	Bounding Boxes (Base)	CLIP-text	CLIP-vision + Faster R-CNN	Generates pseudo-labels for novel classes using pre-trained OVOD.
RegionCLIP [155]	OVOD	Captions	Bounding Boxes (Base + Pseudo Novel)	CLIP-text	CLIP-vision + Faster R-CNN	Creates region-text pairs as pseudo labels using CLIP and pre-train the detector in the first stage.
Detic [156]	OVOD	ImageNet	Bounding Boxes (Base + Pseudo Novel)	CLIP-text	Centernet2	Propose a weakly supervised approach that is training rare classes with image-level annotations.
DetPro [157]	OVOD	ImageNet	Bounding Boxes (Base + Pseudo Novel)	CLIP-text	Centernet2	learn continuous prompt representations for open vocabulary object detection based on the pre-trained vision-language model.
OV-DETR [158]	OVOD	None	Bounding Boxes (Base)	CLIP-text	CLIP-vision + DETR	Introduces a conditional binary matching mechanism to let DETR model generalize to queries from unseen classes.
CORA [159]	OVOD	None	Bounding Boxes (Base)	CLIP-text	CLIP-vision + DETR	Propose Anchor Pre-Matching strategy to reduce both training and inference time for conditional binary matching.
Prompt-OVD [160]	OVOD	None	Bounding Boxes (Base)	CLIP-text	CLIP-vision + DETR	Propose RoI-based masked attention and RoI pruning techniques by utilizing CLIP visual features to improve the novel object classification.
VLDet [35]	OVOD	Captions	Bounding Boxes (Base)	CLIP-text	Faster R-CNN	Aligns image regions with words in captions by a set matching method.
F-VL [161]	OVOD	None	Bounding Boxes (Base)	CLIP-text	CLIP-vision + Mask R-CNN	Train the detector with frozen VLMs and combine scores of joint detection and VLMs.
BARON [162]	OVOD	None	Bounding Boxes (Base)	CLIP-text	Faster R-CNN	Aligning Bag of Regions for Open Vocabulary Object Detection.
OWLv2 [163]	OVOD	None	Bounding Boxes (Base + Pseudo Novel)	CLIP-text	ViT + detection head	Generate pseudo-labels from WebL1 dataset and train the detector with the generated datasets.
MaMMUT [164]	OVOD	Captions	Bounding Boxes (Base + Pseudo Novel)	CLIP-text	ViT + detection head	Joint pre-train with multi-modal tasks to benefit the novel object detection.
Open Vocabulary Segmentation (Sec. 3.3)						
LSeg [15]	OVSS	None	Segmentation Masks (Base)	CLIP-text	ViT	Aligns text embeddings from the VLM model with pixel features.
ZegFormer [165]	OVSS	None	Segmentation Masks (Base)	CLIP-text	CLIP-vision + Query-based former Decoder	Decouple segmentation and classification by generating class-agnostic segment masks then classify each mask.
OpenSeg [37]	OVSS	Captions	Segmentation Masks (Base)	ALIGN	EfficientNet-B7	Performs region-word grounding loss between mask features and word features.
MaskCLIP+ [166]	OVSS	None	Segmentation Masks (Pseudo All)	CLIP-text	CLIP-vision + DeepLabv2	Modifies CLIP so that it can output per-pixel feature maps.
OVSeg [167]	OVSS	Captions	Segmentation Masks (Base + Pseudo All)	CLIP-text	CLIP-vision + MaskFormer	Uses CLIP to match the proposed image regions with nouns in the captions to generate pseudo labels.
GroupVit [168]	OVSS	Captions	None	Transformer Encoder	ViT-S	Leans semantic segmentation only with caption data.
Vil-Seg [169]	OVSS	Captions	None	ViT-B	ViT-B	Leans semantic segmentation without pixel-level annotations using contrastive loss and clustering loss.
TCL [170]	OVSS	Captions	None	CLIP-text	CLIP-vision	Proposes a finer-grained contrastive loss for training without pixel-level annotations.
CGG [38]	OVIS	Captions	Segmentation Masks (Base)	BERT	Mask2Former	Fully exploits caption data using caption grounding and generation.
MaskCLIP [39]	OVPS	None	Segmentation Masks (Base)	CLIP-text	CLIP-vision + Mask2Former	Propose Relative Mask Attention (RMA) modules to adapt cropped images to the pre-trained CLIP model.
ODISE [171]	OVPS	Captions	Segmentation Masks (Base)	CLIP-text	Stable Diffusion	Exploits the vision-language alignment learned by denoising diffusion models.
OVDiff [172]	OVSS	None	None	CLIP-text	Stable Diffusion	Proposes a prototype-based method. Use diffusion models to produce prototypes.
OpenSeed [173]	OVIS	None	Segmentation Masks & Boxes (Base)	UniCL	MaskDINO	Jointly learns from detection and segmentation data.
OVSegmentor [174]	OVSS	Captions	None	BERT	DINO	introduces masked entity completion and cross-image mask constituency objectives to improve training.
Cat-Seg [175]	OVSS	None	Segmentation Masks (Base)	CLIP-text	CLIP-image	Jointly aggregates the image and text embeddings from CLIP to form the segmentation predictions.
SAN [176]	OVSS	None	Segmentation Masks (Base)	CLIP-text	CLIP-vision	Proposes a lightweight side adaptor network to extract the CLIP model's knowledge.

TABLE 2: Feature summarization of current open vocabulary object detection approaches.

Method	Common Features
Knowledge Distillation	Distil the aligned visual-text knowledge of VLM into object detection. Focus on distilling loss design and targe proposal generation.
Region Text Pre-training	Use large-scale and easily available text-image pairs to pre-train a better and universal detector and finetune on the target datasets
Training with More Balanced Data	Adopt extra data or balanced datasets as an augmentation to train the classification head.
Prompting Modeling	Adopt different prompting modeling to better transfer the VLM knowledge into detector.
Region Text Alignment	Design a better region-text alignment method to better align the region visual features (RoIs) into text features of VLM.

coder using human-annotated detection datasets. OWL-ViT [185] removes the final token pooling layer of pre-trained VLMs' image encoder and attaches a lightweight classification head and box regression head to each transformer output token before fine-tuning it on standard detection datasets using bipartite matching loss. Meanwhile, MaMMUT [164] presents a simple text decoder and visual encoder for multimodal pre-training. By designing a two-pass on text decoder, it combines both contrastive and generative learning in one framework. The former is for grounding text visual entities, while the latter learns to generate.

Training with More Balanced Data. Rare and unseen data are common in image classification datasets. Joint training can be used to address this issue. The core idea of these approaches by leveraging more balanced data, including image classification datasets, pseudo labels from image-text data, or extra-related detection data. Detic [156] improves long-tail detection performance with image-level supervision. The classification head of Detic is trained using image-level data from ImageNet21K [186]. During training, the max area proposal from RPN is chosen as

the RoI. The basic insight of Detic is that most classification data are object-centric. Therefore, the maximum area proposal may completely cover an object represented by an image-level class. The mm-ovod [187] method improves upon Detic [156] by utilizing multi-modal text embeddings as the classifier. This approach employs a large language model to create a description of each class name rather than relying on manual prompt templates for generating text-based embeddings. In addition, mm-ovod also generates vision-based embeddings from image exemplars. By fusing the text-based and vision-based embeddings, the multi-modal text embeddings can significantly enhance Detic's performance. To use more data, several methods generate pseudo bounding box annotations from large-scale image-caption pairs. PB-OVD [188] uses Grad-CAM [189] and generates the pseudo-bounding boxes combined with RPN's proposals. The activation map of Grad-CAM is obtained from the alignment between region embeddings and word embeddings that come from pre-trained VLMs. Then the boxes are generated from such map and jointly trained with existing box annotations. Meanwhile, several works

leverage the rich semantics available in recent vision and language models to localize and classify objects in unlabeled images. VL-PLM [154] proposes to train Faster R-CNN as a two-stage class-agnostic proposal generator using a detection dataset without category information. LocOV [190] uses class-agnostic proposals in RPN to train Faster R-CNN by matching the region features and word embeddings from image and caption, respectively. From the data generation view, several works [191], [192], [193] adopt the diffusion model to generate the on-target data for effective training. In particular, X-Paste [191] generates the rare class data to improve the classification ability for existing approaches. It uses an extra segmentation model to provide the foreground object masks and adopt simple copy and paste [194] to augment training data. Recently, several works [163], [195], [196] have explored the self-training approaches to generate large pseudo labels for more balanced learning. OWLv2 [163] presents a self-training pipeline. It generates huge pseudo-box annotations on WebLI [197] dataset and pre-trains a model on such generated dataset. Finally, it fine-tunes this model on a specific OVD dataset. Since the WebLI contains a large vocabulary size, OWLv2 achieves significant gains on LVIS and COCO datasets.

Prompting Modeling. Prompt modeling is an effective technique for adapting foundation models to various domains, such as language modeling [198] and image classification [199], [200]. By incorporating learned prompts into the foundation model, the model can transfer its knowledge to downstream tasks more easily. To generate text embeddings of category names, prompts are fed to the text encoder of pre-trained VLMs. However, negative proposals do not belong to any specific category. To address this issue, DetPro [157] forces the negative proposal to be equally dissimilar to any object class instead of using a background class. PromptDet [36] introduces category descriptions into the prompt and explores the position of the category in the prompt. It also proposes to use cached web data to enhance the novel classes during training. Based on the DETR [4] framework, CORA [159] proposes region prompting and anchor pre-matching. The former reduces the gap between the whole image and region distributions by prompting the region features of the CLIP-based region classifier, while the latter learns generalizable object localization via a class-aware matching mechanism. Prompt-OVD [160] follows the pipeline of OV-DETR [158]. It presents ROI-based masked attention and ROI pruning techniques by utilizing CLIP visual features to improve the novel object classification.

Region Text Alignment. Using language as supervision instead ground truth bounding box is an attractive alternative for open vocabulary object detection. However, obtaining enough object-language annotations is difficult and costly. OV-DETR [158] introduces a transformer-based detector for open vocabulary object detection by replacing the bipartite matching method with a conditional binary matching mechanism. VLDet [35] converts the image into a set of regions and the caption into a set of words and solves the object-language alignment problem using a set matching method. It proposes a simple matching strategy to align caption and vision features. DetCLIPv2 [201] uses ATSS [202] as an object detector and trains it with three datasets: a standard detection dataset, a grounding dataset, and an image-text pairs dataset for word-text alignment. Recently, BARON [162] proposes to align the embedding in bags of different regions rather than only individual regions. It first groups contextually interrelated regions as a bag and treats each region in the bag as a word in a sentence. Then, it sends the bag of regions into the text encoder to get bag-

of-regions embeddings. These bag-of-regions embeddings will align with cropped region embeddings from the image encoder of VLMs. F-VLM [161] finds that the origin CLIP features already have grouping effects. It is a two-branch method similar to ViLD-text [13]. F-VLM uses a CLIP vision encoder as the backbone and applies the VLM feature pooler on the region features from the backbone to get VLM predictions. The final result of F-VLM combines the detection scores and the VLM predictions. RO-ViT [203] builds upon F-VLM [161], which believes that the difference in position embeddings between image-level and region-level is responsible for the gap between vision-language pre-training and open vocabulary object detection. To address this issue, RO-ViT proposes a cropped positional embedding module in VLM that bridges the gap between vision-language pre-training and downstream open vocabulary object detection tasks.

3.3 Open Vocabulary Segmentation

In this section, we review the approaches for open vocabulary segmentation problems. Although segmentation problems can be defined in various ways, such as semantic segmentation or panoptic segmentation, we categorize the methods based on their technical aspects.

Utilizing VLMs to Leverage Recognition Capabilities. VLMs have shown remarkable performance in image classification by learning rich visual and linguistic representations. Therefore, it is natural to extend VLMs to semantic segmentation, which can be seen as a dense classification task. For instance, LSeg [15] aligns the text embeddings of category labels from a VLM language encoder with the dense embeddings of the input image. This enables LSeg to leverage the generalization ability of VLMs and segment objects that are not predefined but depend on the input texts. Following LSeg, several works propose methods to utilize the VLMs for open vocabulary segmentation tasks. Fusioner [204] utilizes self-attention operations to combine visual and language features in a transformer-based framework at an early stage. ZegFormer [165] decouples the problem into a class-agnostic segmentation task and a mask classification task. It uses the label embeddings from a VLM to classify the proposal masks and applies the CLIP-vision encoder to obtain language-aligned visual features for them. After that, more approaches are proposed to extract the rich knowledge in VLMs. SAN [176] attaches a lightweight side network to the pre-trained VLM to predict mask proposals and classification outputs. CAT-Seg [175] jointly aggregates the image and text embeddings of CLIP by fine-tuning the image encoder. Han et al. [205] develop an efficient framework that does not rely on the extra computational burden of the CLIP model. OPSNet [206] proposes several modulation modules to enhance the information exchange between the segmentation model and the VLMs. The modulation modules fuse the knowledge of the learned vision model and VLM, which improves the zero-shot performance in novel classes. MaskCLIP [39] inserts Relative Mask Attention (RMA) modules into a pre-trained CLIP model. It can utilize the CLIP features more efficiently. TagCLIP [207] proposes a trusty token module to explicitly predict pixels that contain objects (both base and novel) before classifying each pixel, which avoids the problem that models tend to misidentify pixels into novel categories.

Learning from Caption Data. Image caption data can provide weak supervision for identifying novel classes, as they expose potential novel category names. Like such approaches in open vocabulary object detection [12], image caption data is also explored

TABLE 3: Feature summarization of current open vocabulary segmentation approaches.

Method	Common Feature
Utilizing VLMs to Leverage Recognition Capabilities.	Design fusion or alignment methods to better fuse VLM knowledge into the existing segmenters.
Learning from Caption Data.	Use extra caption data to ground the objects' visual features with caption data.
Generating Pseudo Labels.	Fully explore the potential of the VLM model to generate better masks to train the segmentation models
Training without Pixel-Level Annotations.	Combine the VLM and different unsupervised approaches to perform unsupervised mask generation or segmentation.
Jointly Learning Several Tasks.	Pre-train on large-scale and easily available text-region pairs datasets or detection using a unified detection and segmentation model.
Adopting Denoising Diffusion Models.	Explore the feature representation of text-to-image diffusion models or utilize the generation ability to augment masks.

in open vocabulary segmentation tasks also explore image caption data. OpenSeg [37] applies a region-word grounding loss between mashich enables it to achieve good zero-shot testing ability on different datasets. CGG [38] combines caption grounding and caption generation losses to fully exploit the knowledge in caption data. It leverages the role of object nouns in visual grounding and the mutual benefits of words in caption generation.

Generating Pseudo Labels. Intuitively, providing the model with more data on novel categories can improve classification performance. MaskCLIP+ [166] modifies the CLIP-vision model by replacing the last pooling layer with a convolution layer, which produces dense feature maps. These feature maps are then used to generate pseudo labels for training a segmentation model. OVSeg [167] matches the proposed image regions with nouns in captions using CLIP to generate pseudo annotations. It also proposes a mask prompt tuning module to help CLIP adapt to masked images without changing their weights. XPM [208] follows a similar pseudo data generation procedure by aligning words in captions with regions in images to generate pseudo instance mask labels.

Training without Pixel-Level Annotations. Despite the absence of annotations on novel objects, most methods still require base mask annotations during training, which are costly and labor-intensive to obtain. To reduce the annotation burden, many recent works explore training segmentation models with merely weak supervision, such as image caption. GroupViT [168] proposes a semantic segmentation framework that leverages a grouping mechanism to automatically merge image patches with the same semantics. It trains the model with a contrastive loss on image-caption pairs and does not need pixel-level annotations. PACL [209] enhances the contrastive loss with a patch alignment objective that aligns the image patches and the CLS token of the captions. ViL-Seg [169] combines both contrastive loss and clustering loss. SegCLIP [210] further introduces a reconstruction loss and a superpixel-based KL loss. To compute the superpixel-based KL loss, it uses an unsupervised graph-based segmentation model [211] to generate pseudo labels. TCL [170] proposes a finer-grained contrastive loss, namely text-grounded contrastive loss, which explicitly aligns captions and regions. The model can segment the region that corresponds to a given text expression during inference. OVSegmentor [174] introduces masked entity completion and cross-image mask constituency tasks to improve the training efficiency. Mask-free OVIS [212] generates pseudo mask annotations with purely image-text pair data to assist the segmentation models.

Jointly Learning Several Tasks. Open vocabulary segmentation encompasses different tasks, including OVSS, OVIS, and OVPS. How to jointly learn multiple segmentation tasks in one model becomes a practical problem. X-Decoder [213] proposes a framework that can handle various tasks, including open vocabulary semantic segmentation, open vocabulary instance segmentation, and open vocabulary panoptic segmentation. It utilized a query-

based segmentation architecture, pre-trains the model on a mixture of segmentation data and image-text pairs, and then fine-tuned or applied in zero-shot settings for downstream tasks. FreeSeg [214] also proposes a generic framework to tackle the three tasks in a unified manner. It designs an adaptive task prompt module and performs test time tuning on the learnable prompts to capture the task-specific features. POMP [215] first trains class prompts at a large vocabulary dataset (Imagenet-21K) and then transfer the prompts into multiple open vocabulary tasks. Moreover, if the model can learn from multiple tasks, it raises the question of whether it can benefit from multi-sourced data, e.g., detection and segmentation data. To handle this question, OpenSeeD [173] jointly learns from segmentation and detection datasets. To bridge the task gap, they propose a decoupled decoding framework, which decodes foreground and background masks separately and generates masks for the bounding box proposals.

Adopting Denoising Diffusion Models. Recently, diffusion-based generative models [216] have achieved remarkable success in text-based image generation suggests. There are mainly two ways to let diffusion models enhance open vocabulary tasks. First, The reality and diversity of the images generated by diffusion models suggest that the intermediate representations in the diffusion models may be highly aligned with natural language vocabularies. Inspired by this, ODISE [171] proposes a framework that leverages the middle representation of the diffusion model. The middle representations contain rich semantic information for both base and novel classes. Thus ODISE can perform open vocabulary segmentation by training a decoder head on the representations. Another way to incorporate diffusion models into the open vocabulary setting is to take advantage of the image and mask generation ability [172], [217], [218]. OVDiff [172] proposes a prototype-based method to tackle open vocabulary semantic segmentation. It uses the diffusion model to generate images for various categories and treat them as prototypes. The method does not need training. During testing, the input images are compared with these generated prototypes, and the best-matching one is the predicted class. Meanwhile, several works [217], [218] use the diffusion model to generate images and masks for the rare classes to augment data. Thus, the segmenter can be trained in a more balanced manner or even totally using generated data.

3.4 Open Vocabulary Video Understanding

In this section, we review open vocabulary learning on video tasks. Most works focus on designing VLM models' temporal fusion or association in various settings, including action recognition and tracking.

Video Classification. Traditional video classification methods usually require large datasets specific to video (e.g., Kinetics [236]). However, annotating video datasets requires very high costs. Using semantic information of label texts from web data may alleviate this deficiency. Building on the success of CLIP in image open vocabulary recognition, ActionCLIP [219] uses

TABLE 4: Representative works summarization and comparison in Sec. 3.4, Sec. 3.5 and Sec. 3.6. **OV-VC** refers to open vocabulary video classification. **OV-3D** refers to open vocabulary 3D recognition.

Method	Task	Vision Training Annotations	Text Model	Vision Model	Highlight
Open Vocabulary Video Understanding (Sec. 3.4)					
ActionCLIP [219]	OV-VC	None	CLIP-text	CLIP-vision + Temporal Pooling	The first work proposes to use CLIP for video understanding.
I-VL [220]	OV-VC	Video Class Label (base)	CLIP-text	CLIP-vision + transformer (temporal fusion)	I-VL provides a simple baseline for adapting CLIP to video understanding.
ViFi-CLIP [221]	OV-VC	Video Class Label (base)	CLIP-text	CLIP-vision (learnable) + Temporal Pooling	ViFi-CLIP indicates that a simple fine-tuning baseline is strong enough.
OVTrack [222]	OV-Tracking	Image Bounding Boxes	CLIP-text	CLIP-vision + Faster R-CNN	OVTrack is the first open vocabulary multi-object tracking method.
MindVLT [48]	OV-VIS	Video Segmentation Masks (base)	CLIP-text	CLIP-vision + Mask2Former + SORT	MindVLT is the first open vocabulary video instance segmentation method.
OpenVIS [223]	OV-VIS	Video Segmentation Masks (base)	CLIP-text	CLIP-vision + Mask2Former	OpenVIS conduct open vocabulary VIS in a two-stage manner.
Open Vocabulary 3D Scene Understanding (Sec. 3.5)					
PointCLIP [224]	OV-3D	None	CLIP-text	CLIP-vision (projected depth map)	PointCLIP uses projected depth for OV 3D recognition.
PointCLIPV2 [225]	OV-3D	None	CLIP-text + GPT-3	CLIP-vision (projected depth map)	PointCLIPV2 generates prompts with LLMs to enhance performance.
ULIP [226]	OV-3D	Point Cloud Label	CLIP-text	Point Cloud Encoder + CLIP-vision	ULIP aligns the 3D encoder and 2D CLIP encoder feature by distillation.
CLIP2 [227]	OV-3D	None	CLIP-text	Point Cloud Encoder + CLIP-vision	CLIP2 leverages real-world point cloud data and CLIP to train the 3D encoder for 3D open vocabulary segmentation.
OpenShape [228]	OV-3D	Point Cloud Label	CLIP-text + GPT-4	Point Cloud Encoder + CLIP-vision	OpenShape builds a large-scale dataset that provides image, point cloud, and text triplets.
OV-3DETCH [229]	OV-3D-OD	Pseudo Labels from 2D Detector	CLIP-text	3DDETR [230]	OV-3DETCH exploits information from two modalities to achieve 3D open vocabulary object detection.
PLA [231]	OV-3D-SS/IS	3D segmentation masks (base)	CLIP-text	sparse-conv UNet [232]	PLA first tackles the 3D open vocabulary scene understanding problem.
OpenScene [233]	OV-3D-SS	None	CLIP-text	3D Encoder + LSeg [15]	OpenScene train a 3D Encoder yielding dense features co-embedded with text and image pixels for open vocabulary semantic segmentation.
RegionPLC [234]	OV-3D-SS/IS	None	CLIP-text	Point Cloud Encoder + CLIP-vision	RegionPLC uses the dense caption of any region to extract more information in CLIP for 3D backbone training.
OpenMask3D [235]	OV-3D-IS	3D segmentation masks (base)	CLIP-text	Point Cloud Encoder + CLIP-vision + SAM [33]	OpenMask3D first generates 3D proposals with 3D Encoder and 2D proposals with SAM. Then they are aggregated into per-mask features for open vocabulary recognition.

knowledge from image-based vision-language pre-training. It adds a temporal fusion layer for the zero-shot capability in video action recognition. A concurrent work I-VL [220] follows a similar paradigm by training the transformer layer on top of a frozen CLIP image encoder and also has a strong zero-shot capability. Another concurrent work, EVL [237], also employs the frozen CLIP for efficient video action recognition. X-CLIP [238] uses a video encoder that leverages the temporal information in the encoder for video recognition. It aligns the feature from the video encoder with the text encoder that is pre-trained on the image-based vision-language pairs (e.g., CLIP). To take advantage of other modalities, MOV [239] further fuses the audio information and the pre-trained CLIP model to build a multi-modal open vocabulary video classification model. Text4Vis [240] focuses on the classifier and proposes to use the CLIP text encoder as the semantic target for video classification. Recently, OpenVCLIP [241] formulates the CLIP-to-video knowledge transfer as a continual learning problem and proposes *Interpolated Weight Optimization* to address the issue. AIM [242] tackles the open vocabulary video classification problem by adding adapt layers on top of the CLIP image encoder. ViFi-CLIP [221] reveals that a simple fine-tuning baseline (image-level feature extraction with CLIP visual encoder following temporal pooling) instead of advanced fusion layers can have a strong performance and further investigates the influence of prompt tuning. ASU [243] explores the use of fine-grained language features extracted by semantic units (e.g., head, arms, balloon, knee bend posture of exercise in the video) to guide the training of video classification. Recent advancement in open vocabulary video classification turns the attention to the language part of the VLM modeling. VicTR [244] introduces *video-conditioned text representations* to optimize the visual and text information jointly. MAXI [245] leverages LLMs to build a text bag for video without annotation by text expansion. The verbs, which are lacking in the realm of image, have the opportunity to participate in video-language modeling.

Object Tracking and Video Instance Segmentation. The object tracking and video instance segmentation can also enjoy the rich knowledge of VLMs to build an open vocabulary tracker based on a close-set tracker. Going beyond the large vocabulary object tracking [246], to tackle the real-world multiple object tracking (MOT), OVTrack [222] first introduces large VLMs to the object

tracking and tackles their proposed open vocabulary MOT (OV-MOT) task. Specifically, OVTrack extracts RoIs via an RPN and uses CLIP for knowledge distillation. A separate tracking head is used for tracking and supervised by pseudo LVIS videos. As for video instance segmentation (VIS), to make the VIS model capable of generalizing to novel classes in the real world, MindVLT [48] adopts a frozen CLIP backbone and proposes an end-to-end method with an open vocabulary classifier for segmenting and tracking unseen categories. It collects a large-vocabulary VIS dataset and tests their MindVLT on it. A concurrent work, OpenVIS [223], also tackles the open vocabulary video instance segmentation task but in a different manner. It generates the class-agnostic mask of instances and leverages the masks to crop raw images to feed into the CLIP visual encoder for calculating class scores.

3.5 Open Vocabulary 3D Understanding

In this section, we review the open vocabulary approaches used in 3D scene understanding tasks. We mainly survey the works for point cloud classification and segmentation, which explores the knowledge of 2D VLMs into 3D.

3D Recognition. The VLM has shown great success in the zero-shot or few-shot learning of 2D images by leveraging a huge amount of image data. However, such internet-scale data is not available for the 3D point cloud. To this extent, extending the open vocabulary mechanism into 3D perception is not trivial since it is hard to collect enough data for point-language contrastive training like what CLIP does in 2D perception. To mitigate the gap, PointCLIP [224] takes the first step to 3D open vocabulary perception. The principle insight behind PointCLIP is that the 3D point cloud can be converted to CLIP-recognizable images. By projecting the 3D point cloud to a 2D plane and extracting visual features from the projected depth map via the CLIP visual encoder, the point cloud feature can be naturally aligned with the language feature extracted by the language encoder. Then, the whole framework is with 3D point cloud zero-shot capability just like 2D images. However, simply projecting the point cloud to depth maps may yield inferior performance. To further improve the performance, rather than directly using the CLIP visual encoder for visual feature extraction of depth map, CLIP2Point [247] aligns the RGB image feature from the CLIP

visual encoder and depth feature from a depth encoder through contrastive learning. Specifically, they collect image-depth pairs to align the from-scratch depth map encoder with the CLIP image encoder at training time and only use the depth map encoder at inference time. Then, the depth feature can be aligned with the language embedding, facilitating the 3D point cloud zero-shot capability with CLIP. Also aiming at improving the performance on PointCLIP [224], PointCLIPV2 [225] focuses on different perspectives and proposes a realistic shape projection scheme along with an LLM-based 3D prompting generation scheme. Although without extra annotations, PointCLIPV2 achieves a significant improvement over PointCLIP [224].

Though projecting the point cloud to depth maps can make it easy to leverage the existing 2D visual encoders pre-trained in the CLIP, it may not exhaustively use the 3D information in the point cloud. Accordingly, beyond the depth map-based methods, ULIP [226] first collects multi-modalities triplets (point cloud, image, and text) for training the 3D backbone. Since CLIP already aligns the language and image encoders, it only needs to align the 3D backbone to the image-language feature space. With only small-scale data, ULIP [226] aligns the 3D feature extracted by the 3D backbone to the CLIP-aligned visual and text feature to enable the zero-shot capability and enhance the standard 3D recognition capability. The advantage of ULIP [226] also includes unifying the three modalities, which may bring more downstream applications such as image-to-3D retrieval. Though ULIP [226] aligns the 3D and 2D and thus enables the native 3D open vocabulary capability, it trains on a small-scale dataset, which limits its performance. CLIP2 [227] resorts to finding training samples from the real world and proposes *Triplet Proxies Collection* scheme for finding instance-level 3D point cloud, 2D image crop, and text triplets for 3D recognition. OpenShape [228] scales up both the dataset and backbone. For the dataset, they build a text-3D shape dataset containing 876k training shapes with over 1k categories. They also explore adopting larger 3D backbones and their performance. As a result, OpenShape [228] drastically enhances the performance on 3D zero-shot capability. LidarCLIP [248] also aligns the 3D and 2D features with a similar approach, but LidarCLIP [248] focuses on the driving scenes. Besides the 3D zero-shot capability, LidarCLIP [248] also shows point cloud captioning and lidar-to-image generation capability with off-the-shelf foundation models.

3D Object Detection. In 3D object detection, the training data is often hard to get, and existing 3D detectors are often trained on very limited classes, which means they are hard to generalize to novel classes. Inspired by the success of 2D open vocabulary detection [156], aiming at taking full use of both image and point cloud modalities for 3D detection, OV-3DETC [229] and OV-3DET [249] proposes to decouple the localization and recognition in point cloud object detection into localization and recognition. For localization, 2D pre-trained detectors can be adopted for training the 3D detector by back-projecting the 2D bounding box and further optimizing by the point cloud. For recognition, they propose aligning the regional features of 3D and 2D encoders with the corresponding text feature. Therefore, during the inference, 3DETC [229] and OV-3DET [249] can generalize to unseen classes with the knowledge in the CLIP.

3D Scene Understanding. In the 3D scene understanding, the same obstacle, lacking training data, also limits the capability of generalization. Sharing similar motivation that there lacks 3D-text pairs for point-language contrastive training, PLA [231] proposes to extract features from multi-view images sampled from a scene

to generate descriptions with pre-trained language models. The descriptions can then be used to extract language features to train 3D backbone-language alignment. With the language-aligned 3D backbone, it is natural to conduct open vocabulary segmentation like with the 2D image. OpenScene [233] proposes to link the 3D features for each point with CLIP features for each pixel. By back-projecting the 2D pixels to 3D space, each point in the point cloud can be ensembled with features of several pixels in different views. The 3D-text co-embedding makes it possible for open vocabulary semantic segmentation. Inspired by MaskCLIP [166], a concurrent work CLIP-FO3D [250] also focuses on 3D semantic segmentation and has a similar approach. It leverages the feature map extracted by the CLIP visual encoder and directly transfers CLIP's knowledge without any extra annotation. A recent work RegionPLC [234] on 3D open vocabulary semantic segmentation considers the benefits of both PLA [231] and OpenScene [233]. It proposes to use the dense caption of any random region to extract more information in CLIP for 3D backbone distillation. Fine-grained dense supervision in RegionPLC [234] beyond view-level or instance-level further improves performance compared to PLA [231]. Different from training 3D backbones like in [231], [233], [234], [250], PartSLIP [251] and SATR [252] directly projecting the 3D point cloud and mesh to 2D plane and uses GLIP [183] to localize and segment. Meanwhile, OpenMask3D [235] mainly focuses on the 3D instance segmentation. It first generates class-agnostic instance mask proposals with the 3D point cloud. Then, OpenMask3D [235] selects views and projects 3D masks into 2D images. The 2D masks are further refined by SAM [33]. Finally, the 2D masks can be fed into the CLIP visual encoder for generating label prediction with the help of the CLIP language encoder. In the driving scene, to mitigate the heavy dependence on the point cloud data annotation and fast generalization to the new scenes, CLIP2Scene [253] proposes to train a 3D network via semantic-driven cross-modal contrastive learning for 3D segmentation. CLIP2Scene [253] also considers spatial-temporal semantic consistency regularization to facilitate training.

3.6 Closely Related Tasks

In this section, we add several closely related tasks to augment open vocabulary learning. We survey the following aspects: class agnostic detection and segmentation, open world object detection, and open-set panoptic segmentation.

• **Class Agnostic Detection and Segmentation.** The goal of class agnostic detection and segmentation is to learn a general region proposal system that can be used in different scenes. For detection, OLN [254] replaces the binary classification head in RPN by predicting the IoU score of foreground objects, which proves the generalization ability on cross-dataset testing. For example, the model trained on COCO shows the localization ability on the LVIS dataset. Open world instance segmentation [255] aims to correctly detect and segment instances whether their categories are in training taxonomy. GGN [256] leverages the bottom-up grouping idea, combining a local pixel affinity measure with instance-level mask supervision, producing a training regimen designed to make the model more generalizable. Meanwhile, from the data augmentation view, MViT [257] combines the Deformable DETR and CLIP text encoder for the open world class-agnostic detection, where the authors build a large dataset by mixing existing detection datasets. For the segmentation domain,

Entity segmentation [258], [259] aims to segment all visual entities without predicting their semantic labels. The goal of such segmentation is to obtain high-quality and generalized segmentation results. Finer-grained entity [259] presents a two-view image crop ensemble method named CropFormer to enhance the fine-grained details. Recently, SAM [33] proposes more generalized prompting methods, including masks, points, boxes, and texts. In particular, the authors build a larger dataset with 1 billion masks following the spirits of CLIP. The SAM achieves zero-shot testing in various segmentation datasets, which are highly generalizable.

- **Open World Object Detection.** Open world recognition [27] requires the model to identify novel categories and label them as ‘unknown.’ Then, the novel categories are progressively annotated. The model learns incrementally with the data and recognizes the newly-annotated categories. Inspired by this setting, open world object detection (OWOD) [260] expands the recognition task to the detection setting. To tackle the proposed problem, the authors propose a novel method that utilizes contrastive clustering and an energy-based unknown identification module. Following this work, OW-DETR [261] introduces an end-to-end transformer-based framework. It consists of three dedicated components, namely, attention-driven pseudo-labeling, novelty classification, and objectness scoring, to explicitly address the OWOD challenge. Meanwhile, open world DETR [262] proposes a two-stage training approach based on Deformable DETR. It focuses on alleviating catastrophic forgetting when the annotations of the unknown classes become available incrementally using knowledge distillation and exemplar replay technologies. PROB [263] proposes a probabilistic objectness head into the OW-DETR to better mine unknown background classes. Recently, researchers [264] propose a new setting, unknown-classified open world object detection (UC-OWOD), which aims to detect and classify unknown instances into different unknown classes. This task is close to the open vocabulary object detection but requires incremental learning.

- **Open-Set Panoptic Segmentation.** Similar to other open-set tasks, open-set panoptic segmentation (OSPS) [265] requires the model to identify novel categories as ‘unknown’ in a panoptic segmentation task. The ‘un’ classes are chosen from the thing classes (foreground objects). The authors apply exemplar theory for novel class discovery. After that, Dual [266] proposes a divide-and-conquer scheme to develop a dual decision process for OSPS. The results indicate that by properly combining a known class discriminator with an additional class-agnostic object prediction head, the OSPS performance can be significantly improved.

4 BENCHMARK RESULTS

This section systematically compares the different settings and methods in each task. For each setting, first, we introduce the datasets used in the evaluation. Next, we present the details of each setting separately. Then, we compare the results in detailed tables. We list the detailed results and settings for reference.

4.1 Open Vocabulary Object Detection

Settings. Open vocabulary object detection methods, such as OVR-CNN [12] and ViLD [13], have primarily focused on the COCO and LVIS datasets. The COCO dataset comprises 80 classes, with 48 considered base classes and 17 treated as novel classes. Any annotations not labeled with base classes are removed

from the training data. Therefore, for open vocabulary object detection using the COCO dataset, there are 107,761 training images containing 665,387 bounding box annotations of base classes and 4,836 test images with 28,538 bounding box annotations of both base and novel categories. On the other hand, the LVIS dataset is designed for long-tail object detection tasks and includes 1203 classes. 866 frequent and common ones serve as base categories, while the remaining rare ones (377) act as novel categories.

Evaluation Metrics. When evaluating open vocabulary object detection, we calculate the box mAP using an IoU threshold of 0.5 for the COCO dataset and mask mAP for the LVIS dataset. To assess a method’s ability to detect novel classes, we split the *AP* metric into two categories: AP_{novel} and AP_{base} . Our main focus is on measuring AP_{novel} .

Results Comparison. In Tab. 5 & 6, we present the performance of current open vocabulary object detection methods on COCO and LVIS. BARON [162] outperforms other models on both datasets when using Faster R-CNN detector with the ResNet-50 backbone, achieving a high score of 42.7 AP_{novel} on COCO and 22.6 AP_r on LVIS. FVLM [161] achieves 28.0 AP_{novel} on the COCO dataset and 18.6 AP_r on LVIS using only frozen backbone and detection data. When utilizing the ResNet50x64 backbone, FVLM achieves a remarkable performance of 32.8 AP_r on the LVIS dataset, surpassing other methods that employ the Swin-B backbone and additional data like CC3M and ImageNet. And for one-stage detector methods such as HierKD [153] and GridCLIP [268], there is still a significant gap compared to two-stage detectors.

4.2 Open Vocabulary Semantic Segmentation

Settings. There are two main settings in open vocabulary semantic segmentation, according to different train/test data choices.

- 1) **Self-evaluation setting.** Methods like ZegFormer [165] and MaskCLIP+ [166] train and test their models on the train/test split from the same dataset. For example, ZegFormer trains on base annotations on the COCO-Stuff training set and tests on the COCO-Stuff validation set with base and novel categories.
- 2) **Cross-evaluation setting.** Methods like OpenSeg [37] and OVSeg [167] train their models on COCO-Stuff and test on other datasets, such as ADE20K, Pascal VOC, and Pascal Context. There is also another setting that splits a dataset into multiple folds and performs n-fold evaluations. We do not compare the results under this setting considering only few works adopt it [15], [204].

The most commonly used datasets for the cross-evaluation setting are ADE20K, Pascal Context, and Pascal VOC. The ADE20K dataset has 2k validation images that comprise various indoor and outdoor semantic categories. The full dataset contains 2,693 foreground and background classes. Open vocabulary works often evaluate their models with the 847 classes split, named A-847, and the 150 classes split, named A-150. The Pascal Context dataset has 5k validation images with 459 categories (PC-459). Some works also evaluate their models on the dataset with the 59 most frequent classes (PC-59). The Pascal VOC dataset has 20 classes used for evaluation, denoted as PAS-20. OpenSeg [37] proposes only assigning pixels with a Pascal Context category to background classes. We denote this setting as PAS-20^b.

Evaluation Metrics. We adopt mean Intersection-over-Union (mIoU) to evaluate a model’s performance on open vocabulary semantic segmentation. Specifically, for the cross-evaluation setting,

TABLE 5: Open vocabulary object detection results on the COCO dataset. The evaluation metric is box mAP at IoU threshold 0.5 for novel and base classes, respectively. The best results are emphasized in **bold**.

Method	Vision Backbone	Text Model	Trainable Backbone	Detector	Extra Data	AP _{novel}	AP _{base}	AP _{all}
OVR-CNN [12] (CVPR '21)	R50-C4	BERT	✓	Faster R-CNN	COCO Cap	22.8	46.0	39.9
ViLD-ens [13] (ICLR '22)	R50-FPN	CLIP ViT-B/32	✓	Mask R-CNN	-	27.6	59.5	51.3
RegionCLIP [155] (CVPR '22)	R50-C4	CLIP RN50	✓	Faster R-CNN	COCO Cap	26.8	54.8	47.5
RegionCLIP [155] (CVPR '22)	R50-C4	CLIP RN50	✓	Faster R-CNN	CC3M	31.4	57.1	50.4
Detic [156] (ECCV '22)	R50-FPN	CLIP	✓	CenterNet2	IN-L	27.8	47.1	45.0
PB-OVD [188] (ECCV '22)	R50-FPN	CLIP ViT-B/32	✓	Mask R-CNN	COCO Cap	30.8	46.1	42.1
HierKD [153] (CVPR '22)	R50-FPN	CLIP	✓	ATSS	COCO Cap	20.3	51.3	43.2
LocOV [190] (GCPR '22)	R50-FPN	CLIP	✓	Faster R-CNN	COCO Cap	28.6	51.3	45.7
OV-DETR [158] (ECCV '22)	R50-C4	CLIP	✓	Deformable DETR	-	29.4	52.7	61.0
MEDet [267] (arXiv '22)	R50-FPN	CLIP	✓	Faster R-CNN	COCO Cap	32.6	53.5	48.0
PromptDet [36] (ECCV '22)	R50-FPN	CLIP	✓	Mask R-CNN	LAION	31.4	29.1	29.7
VLDet [35] (ICLR '23)	R50-FPN	CLIP	✓	CenterNet2	COCO Cap	32.0	50.6	45.8
F-VLM [161] (ICLR '23)	R50-FPN	CLIP	✗	Mask R-CNN	-	28.0	-	39.6
BARON [162] (CVPR '23)	R50-FPN	CLIP	✓	Faster R-CNN	-	34.0	60.4	53.5
OADP [178] (CVPR '23)	R50-C4	CLIP	✓	Faster R-CNN	COCO Cap	30.0	53.3	47.2
CxORA [159] (CVPR '23)	R50	CLIP	✗	DAB-DETR	-	35.1	35.5	35.4
RO-ViT [203] (CVPR '23)	ViT-B	CLIP	✗	Mask R-CNN	-	30.2	-	41.5

TABLE 6: Open vocabulary object detection results on LVIS 1.0 dataset. The evaluation metric is mask mAP following COCO [5].

Method	Vision Backbone	Text Model	Trainable Backbone	Detector	Extra Data	AP _r	AP _c	AP _f	AP _{all}
ViLD-ens [13] (ICLR'22)	R50-FPN	CLIP ViT-B/32	✓	Mask R-CNN	-	16.6	24.6	30.3	25.5
RegionCLIP [155] (CVPR'22)	R50-C4	CLIP RN50	✓	Faster R-CNN	CC3M	17.1	27.4	34.0	28.2
Detic [156] (ECCV'22)	R50-FPN	CLIP	✓	CenterNet2	IN-L	19.5	-	-	30.9
OV-DETR [158] (ECCV'22)	R50-C4	CLIP	✓	Deformable DETR	-	17.4	25.0	32.5	26.6
MEDet [267] (arXiv'22)	R50-FPN	CLIP	✓	Faster R-CNN	CC3M	22.4	-	-	34.4
DetPro [157] (ECCV'20)	R50-FPN	CLIP ViT-B/32	✓	Mask R-CNN	-	19.8	25.6	28.9	25.9
PromptDet [36] (ECCV'22)	R50-FPN	CLIP	✓	Mask R-CNN	LAION	21.4	23.3	29.3	25.3
VLDet [35] (ICLR'23)	R50-FPN	CLIP	✓	CenterNet2	CC3M	21.7	29.8	34.3	30.1
F-VLM [161] (ICLR'23)	R50-FPN	CLIP	✗	Mask R-CNN	-	18.6	-	-	24.2
BARON [162] (CVPR'23)	R50-FPN	CLIP	✓	Faster R-CNN	-	22.6	27.6	29.8	27.6
OADP [178] (CVPR'23)	R50-C4	CLIP	✓	Faster R-CNN	-	21.7	26.3	29.0	26.6
GridCLIP [268] (arXiv'23)	RN50	ViT-B/32	✓	FCOS	-	15.0	22.7	32.5	25.2
CORA [159] (CVPR'23)	R50	CLIP	✗	DAB-DETR	-	22.2	-	-	-
RO-ViT [203] (CVPR'23)	ViT-B	CLIP	✗	Mask R-CNN	-	28.0	-	-	30.2
RegionCLIP [155] (CVPR'22)	R50x64-C4	CLIP RN50x64	✓	Faster R-CNN	CC3M	22.0	32.1	36.9	32.3
Detic [156] (ECCV'22)	Swin-B	CLIP	✓	CenterNet2	IN-L	23.9	40.2	42.8	38.4
VLDet [35] (ICLR'23)	Swin-B	CLIP	✓	CenterNet2	CC3M	26.3	39.4	41.9	38.1
F-VLM [161] (ICLR'23)	R50x64-FPN	CLIP	✗	Mask R-CNN	-	32.8	-	-	34.9

TABLE 7: Open vocabulary semantic segmentation performances under the self-evaluation setting. The metric is mIoU. “Harmonic” means the harmonic mean of the mIoU for base classes and the mIoU for novel classes.

Method	Backbone	VLM	COCO-Stuff			PASCAL-VOC			PASCAL-Context		
			Base	Novel	Harmonic	Base	Novel	Harmonic	Base	Novel	Harmonic
ZegFormer [165] (CVPR'22)	RN-50	CLIP-ViT-B/16	37.4	21.4	27.2	-	-	-	-	-	-
PA Ding [32] (CVPR'23)	RN-50	CLIP-ViT-B/16	40.4	24.8	30.7	-	-	-	-	-	-
ZegFormer [165] (CVPR'22)	RN-101	CLIP-ViT-B/16	36.6	33.2	34.8	86.4	63.6	73.3	-	-	-
Xu et al. [269] (ECCV'22)	RN-101	CLIP-ViT-B/16	39.6	43.6	41.5	79.2	78.1	79.3	-	-	-
PA Ding* [32] (CVPR'23)	RN-101	CLIP-ViT-B/16	39.9	44.9	42.2	-	-	-	-	-	-
MaskCLIP+ [166] (ECCV'22)	RN-101	CLIP-RN-50	39.6	54.7	45.0	88.1	86.1	87.4	48.1	66.7	53.3
FreeSeg [214] (CVPR'23)	RN-101	CLIP-ViT-B/16	42.2	49.1	45.3	91.8	82.6	86.9	-	-	-

the IoU averaged on all the categories in the evaluation datasets is listed because all the classes can be seen as novel. For the self-evaluation setting, the testing dataset usually contains both base and novel classes. For a fair comparison, we only report mIoUs on novel classes while highlighting that the number is in a different setting.

Results under the Self-evaluation Setting. Tab. 7 shows the open vocabulary semantic segmentation results under the self-evaluation setting. MaskCLIP+ [166] achieves the highest novel

mIoU on COCO-Stuff, PASCAL-VOC, and PASCAL-Context, while in general, FreeSeg [214] has the best scores on base and harmonic mIoU. PADing* means including complicated crop-mask image preprocess (CLIP-Image encoder).

Results under the Cross-evaluation Setting. Tab. 8 shows the open vocabulary semantic segmentation results under the cross-evaluation setting. UOVN [176] with RN-50 as its visual backbone achieves the highest mIoU of 13.5 on the A-847 dataset. SAN [176] achieves 32.1 on the A-150 dataset. CAT-

TABLE 8: Open vocabulary semantic segmentation performances under the cross-evaluation setting. The metric is mIoU. For COCO, different methods use different supervision to train their models, including mask, classification (cls), and caption (cap). PAS-20^b is an evaluation setting using the PASCAL-VOC dataset proposed by OpenSeg [37]. It only assigns the background class in PASCAL-VOC to the pixels having a PC-59 category, which is harder than PAS-20 in general. “†” means the results are from a re-implementation of CAT-Seg [175]. “**” means the result is only tested on the novel classes in the class split.

Method	Backbone	VLM	COCO			Extra data	A-847	PC-459	A-150	PC-59	PAS-20 ^b	PAS-20
			mask	cls	cap							
MaskCLIP [39] (ECCV'22)	RN-50	CLIP-ViT-L/14	✓	✓	✗	None	8.2	10.0	23.7	45.9	-	-
ZegFormer† [165] (CVPR'22)	RN-101	CLIP-ViT-B/16	✓	✓	✗	None	5.6	10.4	18.0	45.5	65.5	89.5
LSeg+ [37] (ECCV'22)	RN-101	ALIGN	✓	✓	✗	None	2.5	5.2	13.0	36.0	59.0	-
OpenSeg [37] (ECCV'22)	RN-101	ALIGN	✓	✗	✓	Localized Narrative	4.4	7.9	17.5	40.1	63.8	-
Xu et al. [269] (ECCV'22)	RN-101	CLIP-ViT-B/16	✓	✓	✗		7.0	-	20.5	47.7	-	88.4
OVSeg [167] (CVPR'23)	RN-101C	CLIP-ViT-B/16	✓	✓	✓		7.1	11.0	24.8	53.3	-	92.6
Han et al. [205] (ICCV'23)	RN-101	CLIP-RN-50	✓	✓	✓	None	3.5	7.1	18.8	45.2	83.2	-
CAT-Seg [175] (arXiv'23)	RN-101	CLIP-ViT-B/16	✓	✓	✗	None	8.4	16.6	27.2	57.5	78.3	93.7
GroupViT [168] (CVPR'22)	ViT-S/16	None	✗	✗	✗	CC12M + YFCC	-	-	-	22.4	-	52.3
ViL-Seg [169] (ECCV'22)	ViT-B/16	None	✗	✗	✗		-	-	-	16.3*	-	34.4*
OVSegmentor [174] (CVPR'23)	ViT-B/16	None	✗	✗	✗		-	-	-	20.4	-	53.8
TCL [170] (CVPR'23)	ViT-B/16	CLIP-ViT-B/16	✗	✗	✗	CC4M + CC12M	-	-	17.1	33.9	55.0	83.2
SegCLIP [210] (ICML'23)	ViT-B/16	CLIP-ViT-B/16	✗	✗	✓		-	-	-	24.7	-	52.6
PACL [209] (CVPR'23)	ViT-B/16	CLIP-ViT-B/16	✗	✗	✗		-	-	31.4	50.1	-	72.3
OpenSeg [37] (ECCV'22)	Eff-B7	ALIGN	✓	✗	✓	Localized Narrative	8.1	11.5	26.4	44.8	70.2	-
ODISE-cap [171] (CVPR'23)	Stable diffusion	CLIP-ViT-L/14	✓	✗	✓		11.0	13.8	28.7	55.3	82.7	-
ODISE [171] (CVPR'23)	Stable diffusion	CLIP-ViT-L/14	✓	✓	✗		11.1	14.5	29.9	57.3	84.6	-
OVSeg [167] (CVPR'23)	Swin-B	CLIP-ViT-L/14	✓	✓	✓	None	9.0	12.4	29.6	55.7	-	94.5
SAN [176] (CVPR'23)	ViT-L/14	CLIP-ViT-L/14	✓	✓	✗	None	12.4	15.7	32.1	57.7	-	94.6
CAT-Seg [175] (arXiv'23)	Swin-B	CLIP-ViT-L/14	✓	✓	✗	None	10.8	20.4	31.5	62.0	81.8	96.6
X-Decoder [213] (CVPR'23)	DaViT-L	None	✓	✓	✓	[270], [271], [272], [273]	9.2	16.1	29.6	64.0	-	97.7
OpenSeed [173] (ICCV'23)	Swin-L	None	✓	✓	✗		-	-	23.4	-	-	-
HIPIE [275] (arXiv'23)	ViT-H	None	✓	✓	✗		-	-	29.0	-	-	-
UOVN [276] (arXiv'23)	RN-50	None	✓	✓	✗	[272], [277], [278], [279]	13.5	17.1	30.7	54.3	-	-

Seg [175] with Swin-B as its visual backbone has the best mIoU score of 20.4 on the PC-459 dataset. X-Decoder [213] achieves 65.1 and 97.9 on PC-59 and PAS-20 datasets. For the PAS-20^b dataset, ODISE [171] achieves the highest mIoU of 84.6. Note that the works at the bottom blank use large-scale extra data for training. For example, X-Decoder [213] uses Conceptual Captions [270], SBU Captions [271], Visual Genome [272], and COCO Captions [273] as its training set. It contains 4M image-text pairs. Among works training without pixel-level annotations, PACL [209] achieves a much higher score than others. It uses the biggest extra training data that contains CC3M, CC12M, and YFCC.

4.3 Open Vocabulary Instance Segmentation

Settings. Following previous works [12], [38], [208], we adopt two settings in evaluating open vocabulary instance segmentation. **1) Constrained setting.** The base and novel categories are evaluated separately. **2) Generalized setting.** The base and novel categories are evaluated together. Concretely, in the generalized setting, all the category names are input to the model. The model needs to not only classify novel classes but also to distinguish novel classes from base ones. The second setting is harder than the first one.

Evaluation Metrics We adopt mask mean Average Precision (mAP) as the evaluation metric. For the constrained setting, we report AP_{base} and AP_{novel} separately. For the generalized setting, we report mAP for the base, novel, and all classes.

Results on COCO. Tab. 9 shows the open vocabulary instance segmentation results on the COCO dataset. The CGG method [38] achieves the best results on both constrained and generalized settings while not using pre-trained VLMs or any extra data. And Mask-free OVIS [212] gets a relatively high score on novel classes without any mask labels.

4.4 Open Vocabulary Panoptic Segmentation

Settings. The models are trained using COCO-Panoptic, and tested on other datasets in a zero-shot manner. We report both results evaluated on the ADE20K and COCO datasets.

Evaluation Metrics Following previous works [38], [171], [206], we mainly adopt Panoptic Quality (PQ), Segmentation Quality (SQ), and Recognition Quality (RQ) as the evaluation metrics.

Results. Tab. 10 shows the results on the ADE20K dataset. ODISE-cap [171] achieves the best PQ score of 23.4. It surpasses the second-best score by 0.8. Tab. 11 shows the results on the COCO dataset. PADing [32] achieves a better PQ of 41.5 for seen classes, while Freeseg [214] achieves the highest PQ score of 29.8 for unseen classes.

5 CHALLENGES AND OUTLOOK

This section provides a short discussion for future research directions that can facilitate and envision the development of open vocabulary learning.

Explore Temporal Information. In practical applications, video data is readily available and used more frequently. Accurately segmenting and tracking objects that are not predetermined requires a great deal of attention, which is necessary for a wide range of real-world scenarios, such as short video clips and autonomous vehicles. However, there are only a few works [222] exploring open vocabulary learning on detection and tracking in video. Moreover, the input scenes [48] are simple. For example, several clips only contain a few instances, which makes the current tracking solution more trivial. Thus, a more dynamic, challenging video dataset is needed to fully explore the potential of vision language models for open vocabulary learning.

3D Open Vocabulary Scene Understanding. Compared with image and video, point cloud data are more expensive to annotate, in particular for dense prediction tasks. Thus, research on 3D open vocabulary scene understanding is more urgent. Current solutions

TABLE 9: **Open vocabulary instance segmentation** performances on the COCO-Instances dataset.

Method	Backbone	VLM	COCO			Extra data	Constrained		Generalized		
			mask	cls	cap		AP_{base}	AP_{novel}	AP_{base}	AP_{novel}	AP_{all}
D ² Zero [88] (CVPR'23)	RN-50	CLIP-ViT-B/16	✓	✓	✗	None	-	23.7	40.9	21.9	-
XPM [208] (CVPR'22)	RN-50	None	✓	✓	✓	CC3M	42.4	24.0	41.5	21.6	36.3
Mask-free OVIS [212] (CVPR'23)	RN-50	ALBEF	✗	✗	✓	None	-	27.4	-	25.0	-
CGG [38] (ICCV'23)	RN-50	None	✓	✓	✓	None	46.8	29.5	46.0	28.4	41.4

TABLE 10: **Open vocabulary panoptic segmentation** performances on the ADE20K dataset. No methods use extra data for training.

Method	Backbone	VLM	COCO			PQ	PQ^{th}	PQ^{st}	SQ	RQ
			mask	cls	cap					
MaskCLIP [39] (ECCV'22)	RN-50	CLIP-ViT-L/14	✓	✓	✗	15.1	13.5	18.3	70.5	19.2
ODISE [171] (CVPR'23)	Stable diffusion	CLIP-ViT-L/14	✓	✓	✗	22.6	-	-	-	-
ODISE-cap [171] (CVPR'23)	Stable diffusion	CLIP-ViT-L/14	✓	✗	✓	23.4	-	-	-	-
OPSNet [280] (ICCV'23)	Swin-L	CLIP-RN-50	✓	✓	✗	17.7	15.6	21.9	54.9	21.6

TABLE 11: **Open vocabulary panoptic segmentation** performances on the COCO dataset. No methods use extra data for training.

Method	Backbone	VLM	COCO			PQ ^s	SQ ^s	RQ ^s	PQ ^u	SQ ^u	RQ ^u
			mask	cls	cap						
PADing [32] (CVPR'23)	RN-50	CLIP-ViT-B/16	✓	✓	✗	41.5	80.6	49.7	15.3	72.8	18.4
Freeseq [214] (CVPR'23)	RN-101	CLIP-ViT-B/16	✓	✓	✗	31.4	78.3	38.9	29.8	79.2	37.6

for 3D open vocabulary scene understanding focus on designing projection functions for better usage of 2D VLMs. More new solutions for aligning 2D models knowledge into 3D models will be a future direction.

Explore Foundation Models With Specific Adapter For Custom Tasks. Vision foundation models [16], [33] can achieve good zero-shot performance on several standard classification and segmentation datasets. However, for several custom tasks, such as medical image analysis, and aerial images, there are still many corner cases. Thus, designing a task-specific adapter is needed for these custom tasks. Such adapters can fully utilize the knowledge of pre-trained foundation models.

Efficient Training For Target Dataset. As shown in the benchmark section 4, most state-of-the-art methods need huge data for pre-training to achieve good performances. However, the costs are expensive and even unavailable for many research groups to follow. Thus, with the aid of VLM, designing more efficient data learning pipelines or learning methods is more practical and affordable. One possible solution is to adopt the in-context learning [281], [282] to fully explore or connect the knowledge of VLMs and LLMs.

Base Classes Over-fitting Issues. Most approaches detect and segment novel objects by learning proposals from base class annotations. Thus, there are natural gaps in shapes and semantic information between novel objects and base objects. VLM models can bridge such gaps via pre-trained visual-text knowledge. However, most detectors still easily overfit the base classes when both the novel classes have similar shapes and semantics, since these classes are trained with higher confidence scores. More fine-grained feature discriminative modeling [283], [284], [285], including parts or attributes, is required to handle these problems.

Combining with Incremental Learning. In real scenarios, the data annotations are usually open-world and non-stationary, where novel classes may occur continuously and incrementally. However, directly turning into incremental learning may lead to catastrophic forgetting problems. On the other hand, current open world object detection [261] only focuses on novel class localization, rather than classification. How to handle both catastrophic forgetting problems and novel class detection in one framework is worth

exploring in the future.

6 CONCLUSION

This survey offers a detailed examination of the latest developments in open vocabulary learning in computer vision, which appears to be a first of its kind. We provide an overview of the necessary background knowledge, which includes fundamental concepts and introductory knowledge of detection, segmentation, and vision language pre-training. Following that, we summarize more than 50 different models used for various scene understanding tasks. For each task, we categorize the methods based on their technical viewpoint. Additionally, we provide information regarding several closely related domains. In the experiment section, we provide a detailed description of the settings and compare results fairly. Finally, we suggest several future research directions for open vocabulary learning.

Acknowledgement. This work is supported by the National Key Research and Development Program of China (No.2020YFB2103402).

APPENDIX

This section compares the results of different methods of more open vocabulary tasks described in the main paper. We briefly introduce the datasets first and give detailed results for comparison.

.1 Open Vocabulary Video Recognition

Settings. In video classification, existing methods usually test the zero-shot capability on downstream datasets (e.g., UCF and HMDB) pre-trained on Kinetics-400 [236] datasets. In most of the existing methods such as [221], [244], the ground truth of the Kinetics-400 is used for training, while recent method MAXI [245] does not require the ground truth when training on Kinetics-400.

Results Comparison. The comparison results are in Tab.12. Among the existing methods, Open-VCLIP [241] performs best on all three downstream datasets. It is also worth noting that the

TABLE 12: Open vocabulary video classification results. The mean and standard deviation of results are reported.

Method	Vision Backbone	Frames	Ground Truth	UCF101	HMDB51	K600 (Top-1)	K600 (Top-5)
ActionCLIP [219](Arxiv '2109)	ViT-B/16	32	✓	58.3 ± 3.4	40.8 ± 5.4	66.7 ± 1.1	91.6 ± 0.3
I-VL [220](ECCV '22)	ViT-B/16	32	✓	69.3 ± 4.2	44.3 ± 2.2	55.8 ± 0.7	81.4 ± 0.3
X-CLIP [238](ECCV '22)	ViT-B/16	32	✓	72.0 ± 2.3	44.6 ± 5.2	65.2 ± 0.4	86.1 ± 0.8
Text4Vis [240](AAAI '23)	ViT-L/14	16	✓	-	-	68.9 ± 1.0	-
ViFi-CLIP [221](CVPR '23)	ViT-B/16	32	✓	76.8 ± 0.7	51.3 ± 0.6	71.2 ± 1.0	92.2 ± 0.3
ASU [243](Arxiv '2303)	ViT-B/16	32	✓	75.0 ± 3.7	48.1 ± 2.8	67.6 ± 0.2	87.2 ± 0.3
MAXI [245](Arxiv '2303)	ViT-B/16	32	✗	78.2 ± 0.8	52.3 ± 0.7	71.5 ± 0.8	92.5 ± 0.4
VicTR [244](Arxiv '2304)	ViT-B/16	32	✓	72.4 ± 0.3	51.0 ± 1.3	-	-
Open-VCLIP [241](ICML '23)	ViT-B/16	16	✓	83.4 ± 1.2	53.9 ± 1.2	73.0 ± 0.8	93.2 ± 0.1
Open-VCLIP [241](ICML '23)	ViT-L/14	16	✓	87.6 ± 1.2	59.0 ± 0.6	81.1 ± 0.8	96.3 ± 0.3

TABLE 13: The performance comparison on LV-VIS [48] validation and test set. The AP_{all} , AP_{base} , and AP_{novel} mean the average precision of overall categories, base categories, and novel categories.

Method	Backbone	Val			Test		
		mAP_{all}	mAP_{base}	mAP_{novel}	mAP_{all}	mAP_{base}	mAP_{novel}
DetPro [157]-SORT [286]	R50	9.9	14.9	4.1	5.7	8.8	2.8
Detic [156]-SORT [286]	R50	10.1	15.1	4.2	5.7	8.5	3.1
DetPro [157]-OWTB [287]	R50	11.8	17.1	5.7	7.1	9.9	4.0
Detic [156]-OWTB [287]	R50	11.5	16.8	5.3	7.1	10.1	3.8
MindVLT [48]	R50	14.1	18.1	9.4	8.6	10.7	6.4
Detic [156]-SORT [286]	SwinB	14.9	20.7	8.2	11.0	16.2	5.4
Detic [156]-OWTB [287]	SwinB	15.8	21.5	9.1	11.7	16.4	6.6
MindVLT [48]	SwinB	21.4	26.3	15.8	14.9	18.8	10.6

TABLE 14: The performance comparison of zero-shot classification on Objaverse-LVIS [288], ModelNet40 [289], and ScanObjectNN [290].

Method	Training	Objaverse-LVIS [288]			ModelNet40 [289]			ScanObjectNN [290]		
		Top1	Top3	Top5	Top1	Top3	Top5	Top1	Top3	Top5
PointCLIP [224]	None	1.9	4.1	5.8	19.3	28.6	34.8	10.5	20.8	30.6
PointCLIP v2 [225]	None	4.7	9.5	12.9	63.6	77.9	85.0	42.2	63.3	74.5
CG3D [291]		5.0	9.5	11.6	48.7	60.7	66.5	42.5	57.3	60.8
CLIP2Point [247]		2.7	5.8	7.9	49.5	71.3	81.2	25.5	44.6	59.4
ULIP-PointBERT [226]	ShapeNet [292]	6.2	13.6	17.9	60.4	79.0	84.4	51.5	71.1	80.2
OpenShape-SparseConv		11.6	21.8	27.1	72.9	87.2	93.0	52.7	72.7	83.6
OpenShape-PointBERT		10.8	20.2	25.0	70.3	86.9	91.3	51.3	69.4	78.4
ULIP-PointBERT [228]	OpenShape [228]	21.4	38.1	46.0	71.4	84.4	89.2	46.0	66.1	76.4
OpenShape-SparseConv [228]	(w/o Objaverse-LVIS [288])	37.0	58.4	66.9	82.6	95.0	97.5	54.9	76.8	87.0
OpenShape-PointBERT [228]		39.1	60.8	68.9	85.3	96.2	97.4	47.2	72.4	84.7
ULIP-PointBERT [228]	OpenShape [228]	26.8	44.8	52.6	75.1	88.1	93.2	51.6	72.5	82.3
OpenShape-SparseConv [228]		43.4	64.8	72.4	83.4	95.6	97.8	56.7	78.9	88.6
OpenShape-PointBERT [228]		46.8	69.1	77.0	84.4	96.5	98.0	52.2	79.7	88.7

MAXI [245] performs well even without annotations from the Kinetics-400.

Settings. To test the performance of open vocabulary video instance segmentation methods, MindVLT [48] collects LV-VIS datasets inheriting the categories of LVIS [40] and splits the categories into 659 base categories (frequent and common) and 553 novel categories. In the evaluation protocol, the LV-VIS is not used for training but for evaluation only. The mean Average Precision (mAP) is reported for comparison. mAP_{base} and mAP_{novel} refer to mAP for base and novel categories, respectively.

Results Comparison. The comparison results are in Tab.13. Among the methods, MindVLT [48] achieves the best results on both base and novel categories. MindVLT [48] shows stronger improvement in the novel categories.

Settings. For open vocabulary 3D recognition, the zero-shot classification results on three different scale datasets, including ModelNet40 [289], ScanObjectNN [290], and Objaverse-LVIS [288]

are reported. The first two datasets have 40 and 15 common categories, and the Objaverse-LVIS has 1156 LVIS [40] categories. The methods are trained on different datasets but tested on the three datasets for fair comparison.

Results Comparison. As in Tab.14, using the large-scale OpenShape [228] datasets and larger backbones can significantly boost the performance on the downstream testing datasets.

Settings. To test the open vocabulary 3D semantic segmentation methods, two datasets, ScanNet [293] and nuScenes [294], are adopted for covering broad application scenarios. The ScanNet and nuScenes have 19 and 15 categories, respectively. The categories are split into base and novel categories for testing. For example, B15/N4 refers to 15 base categories for training and four novel categories that are missing in the training set. The mIoU^B (base category mIoU), mIoU^N (novel category mIoU), and hIoU (harmonic mIoU) are reported for comparison.

Results Comparison. As in Tab. 15, RegionPLC [234] achieves

TABLE 15: Results for open-world 3D semantic segmentation on ScanNet and nuScenes in terms of hIoU / mIoU^B / mIoU^N. PLA w/o training denotes training without language supervision in [231].

Method	ScanNet [293]			nuScenes [294]	
	B15/N4	B12/N7	B10/N9	B12/N3	B10/N5
LSeg-3D [231]	00.0 / 64.4 / 00.0	00.9 / 55.7 / 00.1	01.8 / 68.4 / 00.9	00.6 / 74.4 / 00.3	0.00 / 71.5 / 0.00
PLA w/o training [231]	39.7 / 68.3 / 28.0	24.5 / 70.0 / 14.8	25.7 / 75.6 / 15.5	25.5 / 75.8 / 15.4	10.7 / 76.0 / 05.7
PLA [231]	65.3 / 68.3 / 62.4	55.3 / 69.5 / 45.9	53.1 / 76.2 / 40.8	47.7 / 73.4 / 35.4	24.3 / 73.1 / 14.5
RegionPLC [234]	69.9 / 68.4 / 71.5	65.1 / 69.6 / 61.1	58.8 / 76.6 / 47.7	62.0 / 75.8 / 52.4	36.6 / 76.7 / 24.1
Fully-Sup (Upper Bound) [234]	73.3 / 68.4 / 79.1	70.6 / 70.0 / 71.8	69.9 / 75.8 / 64.9	73.7 / 76.6 / 71.1	74.8 / 76.8 / 72.8

remarkable performance on novel categories and thus indicates that it has a good capability to generalize to unseen categories.

REFERENCES

- [1] K. He, X. Zhang, S. Ren, and J. Sun, “Deep residual learning for image recognition,” in *CVPR*, 2016. [1](#) [5](#) [6](#)
- [2] K. He, G. Gkioxari, P. Dollár, and R. Girshick, “Mask r-cnn,” in *ICCV*, 2017. [1](#) [5](#) [6](#)
- [3] A. Dosovitskiy, L. Beyer, A. Kolesnikov, D. Weissenborn, X. Zhai, T. Unterthiner, M. Dehghani, M. Minderer, G. Heigold, S. Gelly, J. Uszkoreit, and N. Houlsby, “An image is worth 16x16 words: Transformers for image recognition at scale,” in *ICLR*, 2021. [1](#) [5](#)
- [4] N. Carion, F. Massa, G. Synnaeve, N. Usunier, A. Kirillov, and S. Zagoruyko, “End-to-end object detection with transformers,” in *ECCV*, 2020. [1](#) [5](#) [6](#) [8](#)
- [5] T.-Y. Lin, M. Maire, S. Belongie, J. Hays, P. Perona, D. Ramanan, P. Dollár, and C. L. Zitnick, “Microsoft coco: Common objects in context,” in *ECCV*, 2014. [1](#) [4](#) [13](#)
- [6] B. Romera-Paredes and P. Torr, “An embarrassingly simple approach to zero-shot learning,” in *ICML*, 2015. [1](#)
- [7] A. Bansal, K. Sikka, G. Sharma, R. Chellappa, and A. Divakaran, “Zero-shot object detection,” in *ECCV*, 2018. [1](#)
- [8] Y. Xian, Z. Akata, G. Sharma, Q. Nguyen, M. Hein, and B. Schiele, “Latent embeddings for zero-shot classification,” in *CVPR*, 2016. [1](#)
- [9] J. Devlin, M.-W. Chang, K. Lee, and K. Toutanova, “Bert: Pre-training of deep bidirectional transformers for language understanding,” *arXiv preprint arXiv:1810.04805*, 2018. [1](#) [3](#) [6](#)
- [10] H. Ding, S. Cohen, B. Price, and X. Jiang, “Phraseclick: toward achieving flexible interactive segmentation by phrase and click,” in *ECCV*. Springer, 2020, pp. 417–435. [1](#)
- [11] T. Mikolov, I. Sutskever, K. Chen, G. S. Corrado, and J. Dean, “Distributed representations of words and phrases and their compositionality,” *Advances in neural information processing systems*, vol. 26, 2013. [1](#)
- [12] A. Zareian, K. D. Rosa, D. H. Hu, and S.-F. Chang, “Open-vocabulary object detection using captions,” *CVPR*, 2021. [1](#) [3](#) [6](#) [7](#) [8](#) [12](#) [13](#) [14](#)
- [13] X. Gu, T.-Y. Lin, W. Kuo, and Y. Cui, “Open-vocabulary object detection via vision and language knowledge distillation,” *ICLR*, 2022. [1](#) [3](#) [6](#) [7](#) [8](#) [12](#) [13](#)
- [14] G. Ghiasi, X. Gu, Y. Cui, and T.-Y. Lin, “Open-vocabulary image segmentation,” *ECCV*, 2022. [1](#)
- [15] B. Li, K. Q. Weinberger, S. Belongie, V. Koltun, and R. Ranftl, “Language-driven semantic segmentation,” *arXiv preprint arXiv:2201.03546*, 2022. [1](#) [3](#) [7](#) [8](#) [10](#) [12](#)
- [16] A. Radford, J. W. Kim, C. Hallacy, A. Ramesh, G. Goh, S. Agarwal, G. Sastry, A. Askell, P. Mishkin, J. Clark *et al.*, “Learning transferable visual models from natural language supervision,” in *ICML*, 2021. [2](#) [5](#) [6](#) [15](#)
- [17] C. Jia, Y. Yang, Y. Xia, Y.-T. Chen, Z. Parekh, H. Pham, Q. Le, Y.-H. Sung, Z. Li, and T. Duerig, “Scaling up visual and vision-language representation learning with noisy text supervision,” in *ICML*, 2021. [2](#) [5](#) [6](#)
- [18] Y. Song, T. Wang, S. K. Mondal, and J. P. Sahoo, “A comprehensive survey of few-shot learning: Evolution, applications, challenges, and opportunities,” *arXiv preprint arXiv:2205.06743*, 2022. [2](#)
- [19] Y. Wang, Q. Yao, J. T. Kwok, and L. M. Ni, “Generalizing from a few examples: A survey on few-shot learning,” *ACM computing surveys*, 2020. [2](#)
- [20] W. Wang, V. W. Zheng, H. Yu, and C. Miao, “A survey of zero-shot learning: Settings, methods, and applications,” *ACM TIST*, 2019. [2](#)
- [21] M. Köhler, M. Eisenbach, and H.-M. Gross, “Few-shot object detection: A comprehensive survey,” *arXiv preprint arXiv:2112.11699*, 2021. [2](#)
- [22] P. Xu, X. Zhu, and D. A. Clifton, “Multimodal learning with transformers: A survey,” *arXiv preprint arXiv:2206.06488*, 2022. [2](#)
- [23] T. Baltrušaitis, C. Ahuja, and L.-P. Morency, “Multimodal machine learning: A survey and taxonomy,” *TPAMI*, 2018. [2](#)
- [24] X. Li, H. Ding, W. Zhang, H. Yuan, G. Cheng, P. Jiangmiao, K. Chen, Z. Liu, and C. C. Loy, “Transformer-based visual segmentation: A survey,” *arXiv preprint*, 2023. [2](#)
- [25] L. Ruan and Q. Jin, “Survey: Transformer based video-language pre-training,” *AI Open*, 2022. [2](#)
- [26] A. Bansal, K. Sikka, G. Sharma, R. Chellappa, and A. Divakaran, “Zero-shot object detection,” in *ECCV*, 2018. [2](#)
- [27] A. Bendale and T. Boult, “Towards open world recognition,” in *CVPR*, 2015. [2](#) [12](#)
- [28] X. Sun, H. Ding, C. Zhang, G. Lin, and K.-V. Ling, “M2iosr: Maximal mutual information open set recognition,” *arXiv preprint arXiv:2108.02373*, 2021. [2](#)
- [29] J. Yang, K. Zhou, Y. Li, and Z. Liu, “Generalized out-of-distribution detection: A survey,” *arXiv preprint arXiv:2110.11334*, 2021. [2](#)
- [30] Z. Liu, Y. Lin, Y. Cao, H. Hu, Y. Wei, Z. Zhang, S. Lin, and B. Guo, “Swin transformer: Hierarchical vision transformer using shifted windows,” *arXiv preprint arXiv:2103.14030*, 2021. [2](#)
- [31] H. Zhao, X. Puig, B. Zhou, S. Fidler, and A. Torralba, “Open vocabulary scene parsing,” in *ECCV*, 2017. [3](#)
- [32] S. He, H. Ding, and W. Jiang, “Primitive generation and semantic-related alignment for universal zero-shot segmentation,” in *CVPR*, 2023. [3](#) [4](#) [13](#) [14](#) [15](#)
- [33] A. Kirillov, E. Mintun, N. Ravi, H. Mao, C. Rolland, L. Gustafson, T. Xiao, S. Whitehead, A. C. Berg, W.-Y. Lo, P. Dollár, and R. Girshick, “Segment anything,” 2023. [3](#) [10](#) [11](#) [12](#) [15](#)
- [34] H. Touvron, T. Lavig, G. Izacard, X. Martinet, M.-A. Lachaux, T. Lacroix, B. Rozière, N. Goyal, E. Hambro, F. Azhar, A. Rodriguez, A. Joulin, E. Grave, and G. Lample, “Llama: Open and efficient foundation language models,” *arXiv preprint arXiv:2302.13971*, 2023. [3](#)
- [35] C. Lin, P. Sun, Y. Jiang, P. Luo, L. Qu, G. Haffari, Z. Yuan, and J. Cai, “Learning object-language alignments for open-vocabulary object detection,” *ICLR*, 2023. [3](#) [7](#) [8](#) [13](#)
- [36] C. Feng, Y. Zhong, Z. Jie, X. Chu, H. Ren, X. Wei, W. Xie, and L. Ma, “Promptdet: Towards open-vocabulary detection using uncurated images,” in *ECCV*, 2022. [3](#) [8](#) [13](#)
- [37] G. Ghiasi, X. Gu, Y. Cui, and T.-Y. Lin, “Scaling open-vocabulary image segmentation with image-level labels,” in *ECCV*, 2022. [3](#) [7](#) [9](#) [12](#) [14](#)
- [38] J. Wu, X. Li, H. Ding, X. Li, G. Cheng, Y. Tong, and C. C. Loy, “Betrayed by captions: Joint caption grounding and generation for open vocabulary instance segmentation,” *ICCV*, 2023. [3](#) [7](#) [9](#) [14](#) [15](#)
- [39] Z. Ding, J. Wang, and Z. Tu, “Open-vocabulary panoptic segmentation with maskclip,” *ICML*, 2022. [3](#) [7](#) [8](#) [14](#) [15](#)
- [40] A. Gupta, P. Dollar, and R. Girshick, “Lvis: A dataset for large vocabulary instance segmentation,” in *CVPR*, 2019. [4](#) [16](#)
- [41] J. Wang, P. Zhang, T. Chu, Y. Cao, Y. Zhou, T. Wu, B. Wang, C. He, and D. Lin, “V3det: Vast vocabulary visual detection dataset,” *arXiv preprint arXiv:2304.03752*, 2023. [4](#)
- [42] B. Zhou, H. Zhao, X. Puig, S. Fidler, A. Barriuso, and A. Torralba, “Semantic understanding of scenes through the ADE20K dataset,” *CVPR*, 2017. [4](#)
- [43] M. Everingham, S. A. Eslami, L. Van Gool, C. K. Williams, J. Winn, and A. Zisserman, “The pascal visual object classes challenge: A retrospective,” *IJCV*, 2015. [4](#)
- [44] R. Mottaghi, X. Chen, X. Liu, N.-G. Cho, S.-W. Lee, S. Fidler, R. Urtasun, and A. Yuille, “The role of context for object detection and semantic segmentation in the wild,” in *CVPR*, 2014. [4](#)
- [45] M. Cordts, M. Omran, S. Ramos, T. Rehfeld, M. Enzweiler, R. Benenson, U. Franke, S. Roth, and B. Schiele, “The cityscapes dataset for semantic urban scene understanding,” in *CVPR*, 2016. [4](#)

[46] J. Miao, Y. Wei, Y. Wu, C. Liang, G. Li, and Y. Yang, “Vspw: A large-scale dataset for video scene parsing in the wild,” in *CVPR*, 2021. 4

[47] L. Yang, Y. Fan, and N. Xu, “Video instance segmentation,” in *ICCV*, 2019. 4

[48] H. Wang, S. Wang, C. Yan, X. Jiang, X. Tang, Y. Hu, W. Xie, and E. Gavves, “Towards open-vocabulary video instance segmentation,” in *ICCV*, 2023. 4, 10, 14, 16

[49] H. Ding, C. Liu, S. He, X. Jiang, P. H. Torr, and S. Bai, “MOSE: A new dataset for video object segmentation in complex scenes,” *arXiv preprint arXiv:2302.01872*, 2023. 4, 5

[50] A. Dave, T. Khurana, P. Tokmakov, C. Schmid, and D. Ramanan, “Tao: A large-scale benchmark for tracking any object,” in *ECCV*, 2020. 4

[51] J. Liu, Y. Sun, C. Han, Z. Dou, and W. Li, “Deep representation learning on long-tailed data: A learnable embedding augmentation perspective,” in *CVPR*, 2020. 4

[52] J. Wu, L. Song, T. Wang, Q. Zhang, and J. Yuan, “Forest r-cnn: Large-vocabulary long-tailed object detection and instance segmentation,” in *ACM-MM*, 2020. 4

[53] J. Ren, C. Yu, X. Ma, H. Zhao, S. Yi *et al.*, “Balanced meta-softmax for long-tailed visual recognition,” *NeurIPS*, 2020. 4

[54] J. Tan, C. Wang, B. Li, Q. Li, W. Ouyang, C. Yin, and J. Yan, “Equalization loss for long-tailed object recognition,” in *CVPR*, 2020. 4

[55] S. Zhang, Z. Li, S. Yan, X. He, and J. Sun, “Distribution alignment: A unified framework for long-tail visual recognition,” in *CVPR*, 2021. 4

[56] Y. Li, T. Wang, B. Kang, S. Tang, C. Wang, J. Li, and J. Feng, “Overcoming classifier imbalance for long-tail object detection with balanced group softmax,” in *CVPR*, 2020. 4

[57] T. Wang, Y. Li, B. Kang, J. Li, J. Liew, S. Tang, S. Hoi, and J. Feng, “The devil is in classification: A simple framework for long-tail instance segmentation,” in *ECCV*, 2020. 4

[58] X. Hu, Y. Jiang, K. Tang, J. Chen, C. Miao, and H. Zhang, “Learning to segment the tail,” in *CVPR*, 2020. 4

[59] Y. Zang, C. Huang, and C. C. Loy, “Fasa: Feature augmentation and sampling adaptation for long-tailed instance segmentation,” in *ICCV*, 2021. 4

[60] Y. Li, H. Zhu, Y. Cheng, W. Wang, C. S. Teo, C. Xiang, P. Vadakkepat, and T. H. Lee, “Few-shot object detection via classification refinement and distractor retreatment,” in *CVPR*, 2021. 4

[61] H. Lee, M. Lee, and N. Kwak, “Few-shot object detection by attending to per-sample-prototype,” in *WACV*, 2022. 4

[62] S. Zhang, L. Wang, N. Murray, and P. Koniusz, “Kernelized few-shot object detection with efficient integral aggregation,” in *CVPR*, 2022. 4

[63] Y. Cao, J. Wang, Y. Jin, T. Wu, K. Chen, Z. Liu, and D. Lin, “Few-shot object detection via association and discrimination,” *NeurIPS*, vol. 34, pp. 16 570–16 581, 2021. 4

[64] A. Li and Z. Li, “Transformation invariant few-shot object detection,” in *CVPR*, 2021. 4

[65] A. Wu, S. Zhao, C. Deng, and W. Liu, “Generalized and discriminative few-shot object detection via svd-dictionary enhancement,” *NeurIPS*, 2021. 4

[66] G. Han, Y. He, S. Huang, J. Ma, and S.-F. Chang, “Query adaptive few-shot object detection with heterogeneous graph convolutional networks,” in *ICCV*, 2021. 4

[67] T.-I. Chen, Y.-C. Liu, H.-T. Su, Y.-C. Chang, Y.-H. Lin, J.-F. Yeh, W.-C. Chen, and W. Hsu, “Dual-awareness attention for few-shot object detection,” *TMM*, 2021. 4

[68] L. Zhang, S. Zhou, J. Guan, and J. Zhang, “Accurate few-shot object detection with support-query mutual guidance and hybrid loss,” in *CVPR*, 2021. 4

[69] X. Wang, T. Huang, J. Gonzalez, T. Darrell, and F. Yu, “Frustratingly simple few-shot object detection,” in *ICML*, 2020. 4

[70] L. Qiao, Y. Zhao, Z. Li, X. Qiu, J. Wu, and C. Zhang, “Defrcn: Decoupled faster r-cnn for few-shot object detection,” in *ICCV*, 2021. 4

[71] C. Zhu, F. Chen, U. Ahmed, Z. Shen, and M. Savvides, “Semantic relation reasoning for shot-stable few-shot object detection,” in *CVPR*, 2021. 4

[72] P. Kaul, W. Xie, and A. Zisserman, “Label, verify, correct: A simple few-shot object detection method,” in *CVPR*, 2022. 4

[73] Z. Tian, H. Zhao, M. Shu, Z. Yang, R. Li, and J. Jia, “Prior guided feature enrichment network for few-shot segmentation,” *PAMI*, 2020. 4

[74] H. Ding, H. Zhang, and X. Jiang, “Self-regularized prototypical network for few-shot semantic segmentation,” *Pattern Recognition*, vol. 133, p. 109018, 2023. 4

[75] K. Rakelly, E. Shelhamer, T. Darrell, A. Efros, and S. Levine, “Conditional networks for few-shot semantic segmentation,” *ICLR*, 2018. 4

[76] K. Wang, J. H. Liew, Y. Zou, D. Zhou, and J. Feng, “Panet: Few-shot image semantic segmentation with prototype alignment,” in *ICCV*, 2019. 4

[77] W. Liu, C. Zhang, H. Ding, T.-Y. Hung, and G. Lin, “Few-shot segmentation with optimal transport matching and message flow,” *TMM*, 2021. 4

[78] X. Zhang, Y. Wei, Y. Yang, and T. S. Huang, “Sg-one: Similarity guidance network for one-shot semantic segmentation,” *IEEE transactions on cybernetics*, 2020. 4

[79] Y. Liu, X. Zhang, S. Zhang, and X. He, “Part-aware prototype network for few-shot semantic segmentation,” in *Computer Vision–ECCV 2020: 16th European Conference, Glasgow, UK, August 23–28, 2020, Proceedings, Part IX 16*, 2020. 4

[80] D. A. Ganea, B. Boom, and R. Poppe, “Incremental few-shot instance segmentation,” in *CVPR*, 2021. 4

[81] K. Nguyen and S. Todorovic, “ifs-rnn: An incremental few-shot instance segmenter,” in *CVPR*, 2022. 4

[82] C. Michaelis, I. Ustyuzhaninov, M. Bethge, and A. S. Ecker, “One-shot instance segmentation,” *arXiv preprint arXiv:1811.11507*, 2018. 4

[83] Z. Fan, J.-G. Yu, Z. Liang, J. Ou, C. Gao, G.-S. Xia, and Y. Li, “Fgn: Fully guided network for few-shot instance segmentation,” in *CVPR*, 2020. 4

[84] X. Yan, Z. Chen, A. Xu, X. Wang, X. Liang, and L. Lin, “Meta r-cnn: Towards general solver for instance-level low-shot learning,” in *ICCV*, 2019. 4

[85] Y. Xian, S. Choudhury, Y. He, B. Schiele, and Z. Akata, “Semantic projection network for zero-and few-label semantic segmentation,” in *CVPR*, 2019. 4

[86] H. Zhang and H. Ding, “Prototypical matching and open set rejection for zero-shot semantic segmentation,” in *ICCV*, 2021, pp. 6974–6983. 4

[87] G. Pastore, F. Cermelli, Y. Xian, M. Mancini, Z. Akata, and B. Caputo, “A closer look at self-training for zero-label semantic segmentation,” in *CVPRW*, 2021. 4

[88] S. He, H. Ding, and W. Jiang, “Semantic-promoted debiasing and background disambiguation for zero-shot instance segmentation,” in *CVPR*, 2023. 4, 15

[89] D. Baek, Y. Oh, and B. Ham, “Exploiting a joint embedding space for generalized zero-shot semantic segmentation,” *arXiv:2108.06536*, 2021. 4

[90] M. Bucher, T.-H. Vu, M. Cord, and P. Pérez, “Zero-shot semantic segmentation,” *NeurIPS*, 2019. 4

[91] Z. Gu, S. Zhou, L. Niu, Z. Zhao, and L. Zhang, “Context-aware feature generation for zero-shot semantic segmentation,” in *ACM MM*, 2020. 4

[92] F. Shen, J. Liu, and P. Hu, “Counterfactual generative zero-shot semantic segmentation,” *arXiv:2106.06360*, 2021. 4

[93] A. Joulin, E. Grave, P. Bojanowski, M. Douze, H. Jégou, and T. Mikolov, “Fasttext: zip: Compressing text classification models,” *arXiv:1612.03651*, 2016. 4

[94] T. Mikolov, I. Sutskever, K. Chen, G. S. Corrado, and J. Dean, “Distributed representations of words and phrases and their compositionality,” in *NeurIPS*, 2013. 4

[95] P. Li, Y. Wei, and Y. Yang, “Consistent structural relation learning for zero-shot segmentation,” *NeurIPS*, 2020. 4

[96] Z. Gu, S. Zhou, L. Niu, Z. Zhao, and L. Zhang, “From pixel to patch: Synthesize context-aware features for zero-shot semantic segmentation,” *arXiv:2009.12232*, 2020. 4

[97] G. Tian, S. Wang, J. Feng, L. Zhou, and Y. Mu, “Cap2seg: Inferring semantic and spatial context from captions for zero-shot image segmentation,” in *ACM MM*, 2020. 4

[98] Y. Zheng, J. Wu, Y. Qin, F. Zhang, and L. Cui, “Zero-shot instance segmentation,” in *CVPR*, 2021. 4

[99] H. Ding, H. Zhang, J. Liu, J. Li, Z. Feng, and X. Jiang, “Interaction via bi-directional graph of semantic region affinity for scene parsing,” in *ICCV*, 2021. 4

[100] H. Ding, H. Zhang, C. Liu, and X. Jiang, “Deep interactive image matting with feature propagation,” *IEEE Transactions on Image Processing*, vol. 31, pp. 2421–2432, 2022. 4

[101] C. Yu, J. Wang, C. Peng, C. Gao, G. Yu, and N. Sang, “Learning a discriminative feature network for semantic segmentation,” in *CVPR*, 2018. 5

[102] H. Ding, X. Jiang, B. Shuai, A. Q. Liu, and G. Wang, “Semantic segmentation with context encoding and multi-path decoding,” *TIP*, 2020. 5

[103] C. Peng, X. Zhang, G. Yu, G. Luo, and J. Sun, “Large kernel matters—improve semantic segmentation by global convolutional network,” in *CVPR*, 2017. 5

[104] H. Zhao, J. Shi, X. Qi, X. Wang, and J. Jia, "Pyramid scene parsing network," in *CVPR*, 2017. [5](#)

[105] L.-C. Chen, G. Papandreou, F. Schroff, and H. Adam, "Rethinking atrous convolution for semantic image segmentation," *arXiv:1706.05587*, 2017. [5](#)

[106] H. Ding, X. Jiang, B. Shuai, A. Q. Liu, and G. Wang, "Context contrasted feature and gated multi-scale aggregation for scene segmentation," in *CVPR*, 2018. [5](#)

[107] X. Li, H. Zhao, L. Han, Y. Tong, S. Tan, and K. Yang, "Gated fully fusion for semantic segmentation," in *AAAI*, 2020. [5](#)

[108] X. Li, A. You, Z. Zhu, H. Zhao, M. Yang, K. Yang, and Y. Tong, "Semantic flow for fast and accurate scene parsing," in *ECCV*, 2020. [5](#)

[109] X. Li, J. Zhang, Y. Yang, G. Cheng, K. Yang, Y. Tong, and D. Tao, "Sfnet: Faster, accurate, and domain agnostic semantic segmentation via semantic flow," *ArXiv*, vol. abs/2207.04415, 2022. [5](#)

[110] X. Wang, R. Girshick, A. Gupta, and K. He, "Non-local neural networks," in *CVPR*, 2018. [5](#)

[111] A. Kirillov, Y. Wu, K. He, and R. Girshick, "Pointrend: Image segmentation as rendering," in *CVPR*, 2020. [5](#)

[112] H. Ding, X. Jiang, A. Q. Liu, N. M. Thalmann, and G. Wang, "Boundary-aware feature propagation for scene segmentation," in *ICCV*, 2019. [5](#)

[113] X. Li, X. Li, L. Zhang, G. Cheng, J. Shi, Z. Lin, S. Tan, and Y. Tong, "Improving semantic segmentation via decoupled body and edge supervision," in *ECCV*, 2020. [5](#)

[114] H. He, X. Li, G. Cheng, Y. Tong, and L. Weng, "Boundarysqueeze: Image segmentation as boundary squeezing," 2021. [5](#)

[115] J. Fu, J. Liu, H. Tian, Z. Fang, and H. Lu, "Dual attention network for scene segmentation," in *CVPR*, 2019. [5](#)

[116] H. Hu, J. Gu, Z. Zhang, J. Dai, and Y. Wei, "Relation networks for object detection," in *CVPR*, 2018. [5](#)

[117] S. Ren, K. He, R. Girshick, and J. Sun, "Faster r-cnn: Towards real-time object detection with region proposal networks," *NeurIPS*, vol. 28, 2015. [5, 6](#)

[118] Z. Tian, C. Shen, H. Chen, and T. He, "Fcos: Fully convolutional one-stage object detection," in *ICCV*, 2019. [5](#)

[119] T.-Y. Lin, P. Goyal, R. Girshick, K. He, and P. Dollár, "Focal loss for dense object detection," in *ICCV*, 2017. [5](#)

[120] Z. Tian, C. Shen, and H. Chen, "Conditional convolutions for instance segmentation," in *ECCV*, 2020. [5](#)

[121] D. Neven, B. D. Brabandere, M. Proesmans, and L. V. Gool, "Instance segmentation by jointly optimizing spatial embeddings and clustering bandwidth," in *CVPR*, 2019. [5](#)

[122] B. De Brabandere, D. Neven, and L. Van Gool, "Semantic instance segmentation with a discriminative loss function," *arXiv preprint arXiv:1708.02551*, 2017. [5](#)

[123] K. Chen, J. Pang, J. Wang, Y. Xiong, X. Li, S. Sun, W. Feng, Z. Liu, J. Shi, W. Ouyang, C. C. Loy, and D. Lin, "Hybrid task cascade for instance segmentation," in *CVPR*, 2019. [5](#)

[124] R. Zhang, Z. Tian, C. Shen, M. You, and Y. Yan, "Mask encoding for single shot instance segmentation," in *CVPR*, 2020. [5](#)

[125] D. Bolya, C. Zhou, F. Xiao, and Y. J. Lee, "Yolact: Real-time instance segmentation," in *ICCV*, 2019. [5](#)

[126] S. Qiao, L.-C. Chen, and A. Yuille, "Detectors: Detecting objects with recursive feature pyramid and switchable atrous convolution," in *CVPR*, 2021. [5](#)

[127] B. Cheng, M. D. Collins, Y. Zhu, T. Liu, T. S. Huang, H. Adam, and L.-C. Chen, "Panoptic-deeplab: A simple, strong, and fast baseline for bottom-up panoptic segmentation," in *CVPR*, 2020. [5](#)

[128] X. Wang, R. Zhang, T. Kong, L. Li, and C. Shen, "SOLov2: Dynamic and fast instance segmentation," in *NeurIPS*, 2020. [5](#)

[129] Q. Zhou, X. Li, L. He, Y. Yang, G. Cheng, Y. Tong, L. Ma, and D. Tao, "TransVOD: End-to-end video object detection with spatial-temporal transformers," *PAMI*, 2022. [5](#)

[130] H. Ding, C. Liu, S. Wang, and X. Jiang, "VLT: Vision-language transformer and query generation for referring segmentation," *TPAMI*, 2022. [5](#)

[131] C. Liu, H. Ding, and X. Jiang, "GRES: Generalized referring expression segmentation," in *CVPR*, 2023. [5](#)

[132] X. Li, S. Xu, Y. Yang, G. Cheng, Y. Tong, and D. Tao, "Panopticpartformer: Learning a unified model for panoptic part segmentation," in *ECCV*, 2022. [5](#)

[133] X. Li, S. Xu, Y. Yang, H. Yuan, G. Cheng, Y. Tong, Z. Lin, M.-H. Yang, and D. Tao, "Panopticpartformer++: A unified and decoupled view for panoptic part segmentation," *arXiv preprint arXiv:2301.00954*, 2023. [5](#)

[134] H. Yuan, X. Li, Y. Yang, G. Cheng, J. Zhang, Y. Tong, L. Zhang, and D. Tao, "Polyphonicformer: Unified query learning for depth-aware video panoptic segmentation," 2021. [5](#)

[135] S. Xu, X. Li, J. Wang, G. Cheng, Y. Tong, and D. Tao, "Fashionformer: A simple, effective and unified baseline for human fashion segmentation and recognition," *ECCV*, 2022. [5](#)

[136] Y. Xu, X. Li, H. Yuan, Y. Yang, J. Zhang, Y. Tong, L. Zhang, and D. Tao, "Multi-task learning with multi-query transformer for dense prediction," *arXiv preprint arXiv:2205.14354*, 2022. [5](#)

[137] X. Li, H. Yuan, W. Zhang, J. Pang, G. Cheng, and C. C. Loy, "Tubelink: A flexible cross tube baseline for universal video segmentation," *arXiv pre-print*, 2023. [5](#)

[138] H. W. Kuhn, "The hungarian method for the assignment problem," *Naval research logistics quarterly*, 1955. [5](#)

[139] H. Wang, Y. Zhu, H. Adam, A. Yuille, and L.-C. Chen, "Max-deeplab: End-to-end panoptic segmentation with mask transformers," in *CVPR*, 2021. [5](#)

[140] W. Zhang, J. Pang, K. Chen, and C. C. Loy, "K-net: Towards unified image segmentation," in *NeurIPS*, 2021. [5](#)

[141] B. Cheng, A. G. Schwing, and A. Kirillov, "Per-pixel classification is not all you need for semantic segmentation," in *NeurIPS*, 2021. [5](#)

[142] H. Wang, Y. Zhu, B. Green, H. Adam, A. Yuille, and L.-C. Chen, "Axial-deeplab: Stand-alone axial-attention for panoptic segmentation," in *ECCV*, 2020. [5](#)

[143] B. Cheng, I. Misra, A. G. Schwing, A. Kirillov, and R. Girdhar, "Masked-attention mask transformer for universal image segmentation," in *CVPR*, 2022. [5](#)

[144] X. Zhu, W. Su, L. Lu, B. Li, X. Wang, and J. Dai, "Deformable {detr}: Deformable transformers for end-to-end object detection," in *ICLR*, 2021. [5, 6](#)

[145] Y. Wu, A. Kirillov, F. Massa, W.-Y. Lo, and R. Girshick, "Detectron2," <https://github.com/facebookresearch/detectron2>, 2019. [5](#)

[146] H. Ding, C. Liu, S. Wang, and X. Jiang, "Vision-language transformer and query generation for referring segmentation," in *ICCV*, 2021. [5](#)

[147] L. H. Li, M. Yatskar, D. Yin, C.-J. Hsieh, and K.-W. Chang, "Visualbert: A simple and performant baseline for vision and language," *arXiv preprint arXiv:1908.03557*, 2019. [5](#)

[148] G. Li, N. Duan, Y. Fang, M. Gong, and D. Jiang, "Unicoder-vl: A universal encoder for vision and language by cross-modal pre-training," in *AAAI*, 2020. [5](#)

[149] J. Lu, D. Batra, D. Parikh, and S. Lee, "Vilbert: Pretraining task-agnostic visiolinguistic representations for vision-and-language tasks," *NeurIPS*, 2019. [5](#)

[150] H. Tan and M. Bansal, "Lxmert: Learning cross-modality encoder representations from transformers," *ACL*, 2019. [5](#)

[151] D. Qi, L. Su, J. Song, E. Cui, T. Bharti, and A. Sacheti, "Imagebert: Cross-modal pre-training with large-scale weak-supervised image-text data," *arXiv preprint arXiv:2001.07966*, 2020. [5](#)

[152] Z. Huang, Z. Zeng, B. Liu, D. Fu, and J. Fu, "Pixel-bert: Aligning image pixels with text by deep multi-modal transformers," *arXiv preprint arXiv:2004.00849*, 2020. [5](#)

[153] Z. Ma, G. Luo, J. Gao, L. Li, Y. Chen, S. Wang, C. Zhang, and W. Hu, "Open-vocabulary one-stage detection with hierarchical visual-language knowledge distillation," in *CVPR*, 2022. [6, 7, 12, 13](#)

[154] S. Zhao, Z. Zhang, S. Schulter, L. Zhao, B. Vijay Kumar, A. Stathopoulos, M. Chandraker, and D. N. Metaxas, "Exploiting unlabeled data with vision and language models for object detection," in *ECCV*, 2022. [7, 8](#)

[155] Y. Zhong, J. Yang, P. Zhang, C. Li, N. C. F. Codella, L. H. Li, L. Zhou, X. Dai, L. Yuan, Y. Li, and J. Gao, "Regionclip: Region-based language-image pretraining," *CVPR*, 2021. [6, 7, 13](#)

[156] X. Zhou, R. Girdhar, A. Joulin, P. Krähenbühl, and I. Misra, "Detecting twenty-thousand classes using image-level supervision," *ECCV*, 2022. [7, 11, 13, 16](#)

[157] Y. Du, F. Wei, Z. Zhang, M. Shi, Y. Gao, and G. C. Li, "Learning to prompt for open-vocabulary object detection with vision-language model," *CVPR*, 2022. [7, 8, 13, 16](#)

[158] Y. Zang, W. Li, K. Zhou, C. Huang, and C. C. Loy, "Open-vocabulary detr with conditional matching," in *ECCV*, 2022. [7, 8, 13](#)

[159] X. Wu, F. Zhu, R. Zhao, and H. Li, "Cora: Adapting clip for open-vocabulary detection with region prompting and anchor pre-matching," *CVPR*, 2023. [7, 8, 13](#)

[160] H. Song and J. Bang, "Prompt-guided transformers for end-to-end open-vocabulary object detection," *arXiv preprint arXiv:2303.14386*, 2023. [7, 8](#)

[161] W. Kuo, Y. Cui, X. Gu, A. J. Piergiovanni, and A. Angelova, "F-vlm: Open-vocabulary object detection upon frozen vision and language models," *ICLR*, 2023. [7, 8, 12, 13](#)

[162] S. Wu, W. Zhang, S. Jin, W. Liu, and C. C. Loy, "Aligning bag of regions for open-vocabulary object detection," in *CVPR*, 2023. [7](#), [8](#), [12](#), [13](#)

[163] M. Minderer, A. A. Gritsenko, and N. Houlsby, "Scaling open-vocabulary object detection," *arxiv*, 2023. [7](#), [8](#)

[164] W. Kuo, A. Piergiovanni, D. Kim, X. Luo, B. Caine, W. Li, A. Ogale, L. Zhou, A. Dai, Z. Chen *et al.*, "Mammut: A simple architecture for joint learning for multimodal tasks," *arXiv preprint arXiv:2303.16839*, 2023. [7](#)

[165] J. Ding, N. Xue, G.-S. Xia, and D. Dai, "Decoupling zero-shot semantic segmentation," in *CVPR*, 2022. [7](#), [8](#), [12](#), [13](#), [14](#)

[166] C. Zhou, C. C. Loy, and B. Dai, "Extract free dense labels from clip," in *ECCV*, 2021. [7](#), [9](#), [11](#), [12](#), [13](#)

[167] F. Liang, B. Wu, X. Dai, K. Li, Y. Zhao, H. Zhang, P. Zhang, P. Vajda, and D. Marculescu, "Open-vocabulary semantic segmentation with mask-adapted clip," *arXiv preprint arXiv:2210.04150*, 2022. [7](#), [9](#), [12](#), [14](#)

[168] J. Xu, S. De Mello, S. Liu, W. Byeon, T. Breuel, J. Kautz, and X. Wang, "Groupvit: Semantic segmentation emerges from text supervision," in *CVPR*, 2022. [7](#), [9](#), [14](#)

[169] Q. Liu, Y. Wen, J. Han, C. Xu, H. Xu, and X. Liang, "Open-world semantic segmentation via contrasting and clustering vision-language embedding," in *ECCV*, 2022. [7](#), [9](#), [14](#)

[170] J. Cha, J. Mun, and B. Roh, "Learning to generate text-grounded mask for open-world semantic segmentation from only image-text pairs," *arXiv preprint arXiv:2212.00785*, 2022. [7](#), [9](#), [14](#)

[171] J. Xu, S. Liu, A. Vahdat, W. Byeon, X. Wang, and S. De Mello, "Open-vocabulary panoptic segmentation with text-to-image diffusion models," *CVPR*, 2023. [7](#), [9](#), [14](#), [15](#)

[172] L. Karazija, I. Laina, A. Vedaldi, and C. Rupprecht, "Diffusion models for zero-shot open-vocabulary segmentation," 2023. [7](#), [9](#)

[173] H. Zhang, F. Li, X. Zou, S. Liu, C. Li, J. Gao, J. Yang, and L. Zhang, "A simple framework for open-vocabulary segmentation and detection," *ICCV*, 2023. [7](#), [9](#), [14](#)

[174] J. Xu, J. Hou, Y. Zhang, R. Feng, Y. Wang, Y. Qiao, and W. Xie, "Learning open-vocabulary semantic segmentation models from natural language supervision," *arXiv preprint arXiv:2301.09121*, 2023. [7](#), [9](#), [14](#)

[175] S. Cho, H. Shin, S. Hong, S. An, S. Lee, A. Arnab, P. H. Seo, and S. Kim, "Cat-seg: Cost aggregation for open-vocabulary semantic segmentation," *arXiv preprint arXiv:2303.11797*, 2023. [7](#), [8](#), [14](#)

[176] M. Xu, Z. Zhang, F. Wei, H. Hu, and X. Bai, "Side adapter network for open-vocabulary semantic segmentation," *CVPR*, 2023. [7](#), [8](#), [13](#), [14](#)

[177] H. Rasheed, M. Maaz, M. U. Khattak, S. Khan, and F. S. Khan, "Bridging the gap between object and image-level representations for open-vocabulary detection," in *NeurIPS*, 2022. [6](#)

[178] L. Wang, Y. Liu, P. Du, Z. Ding, Y. Liao, Q. Qi, B. Chen, and S. Liu, "Object-aware distillation pyramid for open-vocabulary object detection," *CVPR*, 2023. [6](#), [13](#)

[179] H.-C. Cho, W. Y. Jhoo, W. Kang, and B. Roh, "Open-vocabulary object detection using pseudo caption labels," *arXiv preprint arXiv:2303.13040*, 2023. [6](#)

[180] K. Chen, X. Jiang, Y. Hu, X. Tang, Y. Gao, J. Chen, and W. Xie, "Ovarianet: Towards open-vocabulary object attribute recognition," *CVPR*, 2023. [6](#)

[181] G. Patterson and J. Hays, "Coco attributes: Attributes for people, animals, and objects," in *ECCV*, 2016. [6](#)

[182] K. Buettner and A. Kovashka, "Enhancing the role of context in region-word alignment for object detection," *ArXiv*, vol. abs/2303.10093, 2023. [6](#)

[183] L. H. Li*, P. Zhang*, H. Zhang*, J. Yang, C. Li, Y. Zhong, L. Wang, L. Yuan, L. Zhang, J.-N. Hwang, K.-W. Chang, and J. Gao, "Grounded language-image pre-training," in *CVPR*, 2022. [6](#), [11](#)

[184] H. Zhang, P. Zhang, X. Hu, Y.-C. Chen, L. H. Li, X. Dai, L. Wang, L. Yuan, J.-N. Hwang, and J. Gao, "Glipv2: Unifying localization and vision-language understanding," *arXiv preprint arXiv:2206.05836*, 2022. [6](#)

[185] M. Minderer, A. Gritsenko, A. Stone, M. Neumann, D. Weissenborn, A. Dosovitskiy, A. Mahendran, A. Arnab, M. Dehghani, Z. Shen, X. Wang, X. Zhai, T. Kipf, and N. Houlsby, "Simple open-vocabulary object detection with vision transformers," *ECCV*, 2022. [7](#)

[186] O. Russakovsky, J. Deng, H. Su, J. Krause, S. Satheesh, S. Ma, Z. Huang, A. Karpathy, A. Khosla, M. Bernstein *et al.*, "Imagenet large scale visual recognition challenge," *IJCV*, 2015. [7](#)

[187] P. Kaul, W. Xie, and A. Zisserman, "Multi-modal classifiers for open-vocabulary object detection," *ICML*, 2023. [7](#)

[188] M. Gao, C. Xing, J. C. Niebles, J. Li, R. Xu, W. Liu, and C. Xiong, "Open vocabulary object detection with pseudo bounding-box labels," in *ECCV*, 2021. [7](#), [13](#)

[189] R. R. Selvaraju, A. Das, R. Vedantam, M. Cogswell, D. Parikh, and D. Batra, "Grad-cam: Visual explanations from deep networks via gradient-based localization," *IJCV*, 2016. [7](#)

[190] M. A. Bravo, S. Mittal, and T. Brox, "Localized vision-language matching for open-vocabulary object detection," in *GCPR*, 2022. [8](#), [13](#)

[191] H. Zhao, D. Sheng, J. Bao, D. Chen, D. Chen, F. Wen, L. Yuan, C. Liu, W. Zhou, Q. Chu *et al.*, "X-paste: Revisit copy-paste at scale with clip and stablediffusion," *arXiv preprint arXiv:2212.03863*, 2022. [8](#)

[192] Z. Li, Q. Zhou, X. Zhang, Y. Zhang, Y. Wang, and W. Xie, "Guiding text-to-image diffusion model towards grounded generation," *arXiv preprint arXiv:2301.05221*, 2023. [8](#)

[193] J. Xie, W. Li, X. Li, Z. Liu, Y. S. Ong, and C. C. Loy, "Mosaicfusion: Diffusion models as data augmenters for large vocabulary instance segmentation," *ArXiv*, 2023. [8](#)

[194] G. Ghiasi, Y. Cui, A. Srinivas, R. Qian, T.-Y. Lin, E. D. Cubuk, Q. V. Le, and B. Zoph, "Simple copy-paste is a strong data augmentation method for instance segmentation," in *CVPR*, 2021. [8](#)

[195] R. Arandjelović, A. Andonian, A. Mensch, O. J. Hénaff, J.-B. Alayrac, and A. Zisserman, "Three ways to improve feature alignment for open vocabulary detection," *arXiv preprint arXiv:2303.13518*, 2023. [8](#)

[196] S. Xu, X. Li, W. Zhang, S. Wu, G. Cheng, Y. Tong, and C. C. Loy, "Open vocabulary object detection via dynamic self-training," *ArXiv*, 2023. [8](#)

[197] X. Chen, X. Wang, S. Changpinyo, A. Piergiovanni, P. Padlewski, D. Salz, S. Goodman, A. Grycner, B. Mustafa, L. Beyer *et al.*, "Pali: A jointly-scaled multilingual language-image model," *arXiv preprint arXiv:2209.06794*, 2022. [8](#)

[198] T. Brown, B. Mann, N. Ryder, M. Subbiah, J. D. Kaplan, P. Dhariwal, A. Neelakantan, P. Shyam, G. Sastry, A. Askell *et al.*, "Language models are few-shot learners," *NeurIPS*, 2020. [8](#)

[199] R. Zhang, R. Fang, P. Gao, W. Zhang, K. Li, J. Dai, Y. Qiao, and H. Li, "Tip-adapter: Training-free clip-adapter for better vision-language modeling," *arXiv preprint arXiv:2111.03930*, 2021. [8](#)

[200] K. Zhou, J. Yang, C. C. Loy, and Z. Liu, "Learning to prompt for vision-language models," *IJCV*, 2022. [8](#)

[201] L. Yao, J. Han, X. Liang, D. Xu, W. Zhang, Z. Li, and H. Xu, "Detclipv2: Scalable open-vocabulary object detection pre-training via word-region alignment," *CVPR*, 2023. [8](#)

[202] S. Zhang, C. Chi, Y. Yao, Z. Lei, and S. Z. Li, "Bridging the gap between anchor-based and anchor-free detection via adaptive training sample selection," *CVPR*, 2020. [8](#)

[203] D. Kim, A. Angelova, and W. Kuo, "Region-aware pretraining for open-vocabulary object detection with vision transformers," *CVPR*, 2023. [8](#), [13](#)

[204] C. Ma, Y. Yang, Y. Wang, Y. Zhang, and W. Xie, "Open-vocabulary semantic segmentation with frozen vision-language models," *arXiv preprint arXiv:2210.15138*, 2022. [8](#), [12](#)

[205] K. Han, Y. Liu, J. H. Liew, H. Ding, Y. Wei, J. Liu, Y. Wang, Y. Tang, Y. Yang, J. Feng *et al.*, "Global knowledge calibration for fast open-vocabulary segmentation," *ICCV*, 2023. [8](#), [14](#)

[206] X. Chen, S. Li, S.-N. Lim, A. Torralba, and H. Zhao, "Open-vocabulary panoptic segmentation with embedding modulation," *ICCV*, 2023. [8](#), [14](#)

[207] J. Li, P. Chen, S. Qian, and J. Jia, "Tagclip: Improving discrimination ability of open-vocabulary semantic segmentation," 2023. [8](#)

[208] D. Huynh, J. Kuen, Z. Lin, J. Gu, and E. Elhamifar, "Open-vocabulary instance segmentation via robust cross-modal pseudo-labeling," in *CVPR*, 2022. [9](#), [14](#), [15](#)

[209] J. Mukhoti, T.-Y. Lin, O. Poursaeed, R. Wang, A. Shah, P. H. Torr, and S.-N. Lim, "Open vocabulary semantic segmentation with patch aligned contrastive learning," in *CVPR*, 2023. [9](#), [14](#)

[210] H. Luo, J. Bao, Y. Wu, X. He, and T. Li, "Segclip: Patch aggregation with learnable centers for open-vocabulary semantic segmentation," in *ICML*, 2023. [9](#), [14](#)

[211] P. F. Felzenszwalb and D. P. Huttenlocher, "Efficient graph-based image segmentation," *IJCV*, 2004. [9](#)

[212] V. VS, N. Yu, C. Xing, C. Qin, M. Gao, J. C. Niebles, V. M. Patel, and R. Xu, "Mask-free ovis: Open-vocabulary instance segmentation without manual mask annotations," *CVPR*, 2023. [9](#), [14](#), [15](#)

[213] X. Zou, Z.-Y. Dou, J. Yang, Z. Gan, L. Li, C. Li, X. Dai, H. Behl, J. Wang, L. Yuan *et al.*, "Generalized decoding for pixel, image, and language," *CVPR*, 2023. [9](#), [14](#)

[214] J. Qin, J. Wu, P. Yan, M. Li, R. Yuxi, X. Xiao, Y. Wang, R. Wang, S. Wen, X. Pan *et al.*, “Freeseeg: Unified, universal and open-vocabulary image segmentation,” *CVPR*, 2023. [9](#), [13](#), [14](#), [15](#)

[215] S. Ren, A. Zhang, Y. Zhu, S. Zhang, S. Zheng, M. Li, A. Smola, and X. Sun, “Prompt pre-training with twenty-thousand classes for open-vocabulary visual recognition,” 2023. [9](#)

[216] R. Rombach, A. Blattmann, D. Lorenz, P. Esser, and B. Ommer, “High-resolution image synthesis with latent diffusion models,” in *CVPR*, 2022. [9](#)

[217] W. Wu, Y. Zhao, M. Z. Shou, H. Zhou, and C. Shen, “Diffumask: Synthesizing images with pixel-level annotations for semantic segmentation using diffusion models,” *ICCV*, 2023. [9](#)

[218] Z. Li, Q. Zhou, X. Zhang, Y. Zhang, Y. Wang, and W. Xie, “Guiding text-to-image diffusion model towards grounded generation,” *ICCV*, 2023. [9](#)

[219] M. Wang, J. Xing, and Y. Liu, “Actionclip: A new paradigm for video action recognition,” *arXiv pre-print*, 2021. [9](#), [10](#), [16](#)

[220] C. Ju, T. Han, K. Zheng, Y. Zhang, and W. Xie, “Prompting visual-language models for efficient video understanding,” in *ECCV*, 2022. [10](#), [16](#)

[221] H. Rasheed, M. U. Khattak, M. Maaz, S. Khan, and F. S. Khan, “Fine-tuned clip models are efficient video learners,” in *CVPR*, 2023. [10](#), [15](#), [16](#)

[222] S. Li, T. Fischer, L. Ke, H. Ding, M. Danelljan, and F. Yu, “Ovtrack: Open-vocabulary multiple object tracking,” in *CVPR*, 2023. [10](#), [14](#)

[223] P. Guo, T. Huang, P. He, X. Liu, T. Xiao, Z. Chen, and W. Zhang, “Open-VIS: Open-vocabulary video instance segmentation,” *arXiv preprint arXiv:2305.16835*, 2023. [10](#)

[224] R. Zhang, Z. Guo, W. Zhang, K. Li, X. Miao, B. Cui, Y. Qiao, P. Gao, and H. Li, “Pointclip: Point cloud understanding by clip,” in *CVPR*, 2022. [10](#), [11](#), [16](#)

[225] X. Zhu, R. Zhang, B. He, Z. Zeng, S. Zhang, and P. Gao, “Pointclip v2: Adapting clip for powerful 3d open-world learning,” in *ICCV*, 2023. [10](#), [11](#), [16](#)

[226] L. Xue, M. Gao, C. Xing, R. Martín-Martín, J. Wu, C. Xiong, R. Xu, J. C. Niebles, and S. Savarese, “Ulip: Learning unified representation of language, image and point cloud for 3d understanding,” in *CVPR*, 2023. [10](#), [11](#), [16](#)

[227] Y. Zeng, C. Jiang, J. Mao, J. Han, C. Ye, Q. Huang, D.-Y. Yeung, Z. Yang, X. Liang, and H. Xu, “Clip2: Contrastive language-image-point pretraining from real-world point cloud data,” in *CVPR*, 2023. [10](#), [11](#)

[228] M. Liu, R. Shi, K. Kuang, Y. Zhu, X. Li, S. Han, H. Cai, F. Porikli, and H. Su, “Openshape: Scaling up 3d shape representation towards open-world understanding,” *arXiv preprint arXiv:2305.10764*, 2023. [10](#), [11](#), [16](#)

[229] Y. Lu, C. Xu, X. Wei, X. Xie, M. Tomizuka, K. Keutzer, and S. Zhang, “Open-vocabulary 3d detection via image-level class and debiased cross-modal contrastive learning,” *arXiv pre-print*, 2022. [10](#), [11](#)

[230] I. Misra, R. Girdhar, and A. Joulin, “An end-to-end transformer model for 3d object detection,” in *ICCV*, 2021. [10](#)

[231] R. Ding, J. Yang, C. Xue, W. Zhang, S. Bai, and X. Qi, “PLA: Language-driven open-vocabulary 3d scene understanding,” in *CVPR*, 2023. [10](#), [11](#), [17](#)

[232] B. Graham, M. Engelcke, and L. Van Der Maaten, “3D semantic segmentation with submanifold sparse convolutional networks,” in *CVPR*, 2018. [10](#)

[233] S. Peng, K. Genova, C. M. Jiang, A. Tagliasacchi, M. Pollefeys, and T. Funkhouser, “Openscene: 3d scene understanding with open vocabularies,” in *CVPR*, 2023. [10](#), [11](#)

[234] J. Yang, R. Ding, Z. Wang, and X. Qi, “Regionpvc: Regional point-language contrastive learning for open-world 3d scene understanding,” *arXiv preprint arXiv:2304.00962*, 2023. [10](#), [11](#), [16](#), [17](#)

[235] A. Takmaz, E. Fedele, R. W. Sumner, M. Pollefeys, F. Tombari, and F. Engelmann, “Openmask3d: Open-vocabulary 3d instance segmentation,” *arXiv preprint arXiv:2306.13631*, 2023. [10](#), [11](#)

[236] J. Carreira and A. Zisserman, “Quo vadis, action recognition? a new model and the kinetics dataset,” in *CVPR*, 2017. [9](#), [15](#)

[237] Z. Lin, S. Geng, R. Zhang, P. Gao, G. de Melo, X. Wang, J. Dai, Y. Qiao, and H. Li, “Frozen clip models are efficient video learners,” in *ECCV*, 2022. [10](#)

[238] B. Ni, H. Peng, M. Chen, S. Zhang, G. Meng, J. Fu, S. Xiang, and H. Ling, “Expanding language-image pretrained models for general video recognition,” in *ECCV*, 2022. [10](#), [16](#)

[239] R. Qian, Y. Li, Z. Xu, M.-H. Yang, S. Belongie, and Y. Cui, “Multimodal open-vocabulary video classification via pre-trained vision and language models,” *arXiv pre-print*, 2022. [10](#)

[240] W. Wu, Z. Sun, and W. Ouyang, “Revisiting classifier: Transferring vision-language models for video recognition,” in *AAAI*, 2023. [10](#), [16](#)

[241] Z. Weng, X. Yang, A. Li, Z. Wu, and Y.-G. Jiang, “Transforming clip to an open-vocabulary video model via interpolated weight optimization,” in *ICML*, 2023. [10](#), [15](#), [16](#)

[242] T. Yang, Y. Zhu, Y. Xie, A. Zhang, C. Chen, and M. Li, “AIM: Adapting image models for efficient video action recognition,” in *ICLR*, 2023. [10](#)

[243] Y. Chen, D. Chen, R. Liu, H. Li, and W. Peng, “Video action recognition with attentive semantic units,” *arXiv pre-print*, 2023. [10](#), [16](#)

[244] K. Kahatapitiya, A. Arnab, A. Nagrani, and M. S. Ryoo, “VicTR: Video-conditioned text representations for activity recognition,” *arXiv preprint arXiv:2304.02560*, 2023. [10](#), [15](#), [16](#)

[245] W. Lin, L. Karlinsky, N. Shvetsova, H. Possegger, M. Kozinski, R. Panda, R. Feris, H. Kuehne, and H. Bischof, “Match, expand and improve: Unsupervised finetuning for zero-shot action recognition with language knowledge,” *arXiv preprint arXiv:2303.08914*, 2023. [10](#), [15](#), [16](#)

[246] S. Li, M. Danelljan, H. Ding, T. E. Huang, and F. Yu, “Tracking every thing in the wild,” in *ECCV*, 2022. [10](#)

[247] T. Huang, B. Dong, Y. Yang, X. Huang, R. W. Lau, W. Ouyang, and W. Zuo, “Clip2point: Transfer clip to point cloud classification with image-depth pre-training,” *arXiv pre-print*, 2022. [10](#), [16](#)

[248] G. Hess, A. Tonderski, C. Petersson, K. Åström, and L. Svensson, “Lidarclip or: How i learned to talk to point clouds,” *arXiv pre-print*, 2022. [11](#)

[249] Y. Lu, C. Xu, X. Wei, X. Xie, M. Tomizuka, K. Keutzer, and S. Zhang, “Open-vocabulary point-cloud object detection without 3d annotation,” in *CVPR*, 2023. [11](#)

[250] J. Zhang, R. Dong, and K. Ma, “Clip-fo3d: Learning free open-world 3d scene representations from 2d dense clip,” *arXiv pre-print*, 2023. [11](#)

[251] M. Liu, Y. Zhu, H. Cai, S. Han, Z. Ling, F. Porikli, and H. Su, “Part-SLIP: Low-shot part segmentation for 3d point clouds via pretrained image-language models,” in *Proceedings of the IEEE/CVF Conference on Computer Vision and Pattern Recognition*, 2023, pp. 21 736–21 746. [11](#)

[252] A. Abdelreheem, I. Skorokhodov, M. Ovsjanikov, and P. Wonka, “Satr: Zero-shot semantic segmentation of 3d shapes,” *arXiv preprint arXiv:2304.04909*, 2023. [11](#)

[253] R. Chen, Y. Liu, L. Kong, X. Zhu, Y. Ma, Y. Li, Y. Hou, Y. Qiao, and W. Wang, “Clip2scene: Towards label-efficient 3d scene understanding by clip,” in *CVPR*, 2023. [11](#)

[254] D. Kim, T.-Y. Lin, A. Angelova, I. S. Kweon, and W. Kuo, “Learning open-world object proposals without learning to classify,” *RA-L*, 2022. [11](#)

[255] W. Wang, M. Feiszli, H. Wang, and D. Tran, “Unidentified video objects: A benchmark for dense, open-world segmentation,” in *ICCV*, 2021. [11](#)

[256] W. Wang, M. Feiszli, H. Wang, J. Malik, and D. Tran, “Open-world instance segmentation: Exploiting pseudo ground truth from learned pairwise affinity,” *CVPR*, 2022. [11](#)

[257] M. Maaz, H. Rasheed, S. Khan, F. S. Khan, R. M. Anwer, and M.-H. Yang, “Class-agnostic object detection with multi-modal transformer,” in *ECCV*, 2022. [11](#)

[258] L. Qi, J. Kuen, Y. Wang, J. Gu, H. Zhao, P. Torr, Z. Lin, and J. Jia, “Open world entity segmentation,” *TPAMI*, 2022. [12](#)

[259] L. Qi, J. Kuen, W. Guo, T. Shen, J. Gu, W. Li, J. Jia, Z. Lin, and M.-H. Yang, “Fine-grained entity segmentation,” *ICCV*, 2023. [12](#)

[260] K. Joseph, S. Khan, F. S. Khan, and V. N. Balasubramanian, “Towards open world object detection,” in *CVPR*, 2021. [12](#)

[261] A. Gupta, S. Narayan, K. Joseph, S. Khan, F. S. Khan, and M. Shah, “Ow-detr: Open-world detection transformer,” in *CVPR*, 2022. [12](#), [15](#)

[262] N. Dong, Y. Zhang, M. Ding, and G. H. Lee, “Open world detr: Transformer based open world object detection,” *arXiv preprint arXiv:2212.02969*, 2022. [12](#)

[263] O. Zohar, K.-C. Wang, and S. Yeung, “Prob: Probabilistic objectness for open world object detection,” *CVPR*, 2023. [12](#)

[264] Z. Wu, Y. Lu, X. Chen, Z. Wu, L. Kang, and J. Yu, “Uc-owod: Unknown-classified open world object detection,” in *ECCV*, 2022. [12](#)

[265] J. Hwang, S. W. Oh, J.-Y. Lee, and B. Han, “Exemplar-based open-set panoptic segmentation network,” in *CVPR*, 2021. [12](#)

[266] H.-M. Xu, H. Chen, L. Liu, and Y. Yin, “Dual decision improves open-set panoptic segmentation,” in *BMVC*, 2022. [12](#)

[267] P. Chen, K. Sheng, M. Zhang, Y. Shen, K. Li, and C. Shen, “Open vocabulary object detection with proposal mining and prediction equalization,” *arXiv*, 2022. [13](#)

[268] J. Lin and S. Gong, “Gridclip: One-stage object detection by grid-level clip representation learning,” *arXiv*, 2023. [12](#), [13](#)

- [269] M. Xu, Z. Zhang, F. Wei, Y. Lin, Y. Cao, H. Hu, and X. Bai, “A simple baseline for open-vocabulary semantic segmentation with pre-trained vision-language model,” in *ECCV*, 2022. [13](#), [14](#)
- [270] P. Sharma, N. Ding, S. Goodman, and R. Soricut, “Conceptual captions: A cleaned, hypernymed, image alt-text dataset for automatic image captioning,” in *ACL*, 2018. [14](#)
- [271] V. Ordonez, G. Kulkarni, and T. Berg, “Im2text: Describing images using 1 million captioned photographs,” *NeurIPS*, 2011. [14](#)
- [272] R. Krishna, Y. Zhu, O. Groth, J. Johnson, K. Hata, J. Kravitz, S. Chen, Y. Kalantidis, L.-J. Li, D. A. Shamma *et al.*, “Visual genome: Connecting language and vision using crowdsourced dense image annotations,” *IJCV*, 2017. [14](#)
- [273] X. Chen, H. Fang, T.-Y. Lin, R. Vedantam, S. Gupta, P. Dollár, and C. L. Zitnick, “Microsoft coco captions: Data collection and evaluation server,” *CVPR*, 2015. [14](#)
- [274] S. Shao, Z. Li, T. Zhang, C. Peng, G. Yu, X. Zhang, J. Li, and J. Sun, “Objects365: A large-scale, high-quality dataset for object detection,” in *ICCV*, 2019. [14](#)
- [275] X. Wang, S. Li, K. Kallidromitis, Y. Kato, K. Kozuka, and T. Darrell, “Hierarchical open-vocabulary universal image segmentation,” *arXiv preprint arXiv:2307.00764*, 2023. [14](#)
- [276] H. Shi, M. Hayat, and J. Cai, “Unified open-vocabulary dense visual prediction,” *arXiv preprint arXiv:2307.08238*, 2023. [14](#)
- [277] R. Yeh, J. Xiong, W.-M. Hwu, M. Do, and A. Schwing, “Interpretable and globally optimal prediction for textual grounding using image concepts,” *NeurIPS*, 2017. [14](#)
- [278] S. Kazemzadeh, V. Ordonez, M. Matten, and T. Berg, “Referitgame: Referring to objects in photographs of natural scenes,” in *EMNLP*, 2014. [14](#)
- [279] C. Wu, Z. Lin, S. Cohen, T. Bui, and S. Maji, “Phrasicut: Language-based image segmentation in the wild,” in *CVPR*, 2020. [14](#)
- [280] X. Chen, S. Li, S.-N. Lim, A. Torralba, and H. Zhao, “Open-vocabulary panoptic segmentation with embedding modulation,” *ICCV*, 2023. [15](#)
- [281] Z. Fang, X. Li, X. Li, J. M. Buhmann, C. C. Loy, and M. Liu, “Explore in-context learning for 3d point cloud understanding,” *arXiv preprint arXiv:2306.08659*, 2023. [15](#)
- [282] X. Wang, W. Wang, Y. Cao, C. Shen, and T. Huang, “Images speak in images: A generalist painter for in-context visual learning,” *CVPR*, 2023. [15](#)
- [283] P. Sun, S. Chen, C. Zhu, F. Xiao, P. Luo, S. Xie, and Z. Yan, “Going denser with open-vocabulary part segmentation,” *arXiv preprint arXiv:2305.11173*, 2023. [15](#)
- [284] L. Qi, J. Kuen, W. Guo, J. Gu, Z. Lin, B. Du, Y. Xu, and M.-H. Yang, “Aims: All-inclusive multi-level segmentation,” *arXiv preprint arXiv:2305.17768*, 2023. [15](#)
- [285] T.-Y. Pan, Q. Liu, W.-L. Chao, and B. Price, “Towards open-world segmentation of parts,” in *CVPR*, 2023. [15](#)
- [286] N. Wojke, A. Bewley, and D. Paulus, “Simple online and realtime tracking with a deep association metric,” in *ICIP*, 2017. [16](#)
- [287] Y. Liu, I. E. Zulfiqar, J. Luiten, A. Dave, D. Ramanan, B. Leibe, A. Osep, and L. Leal-Taixé, “Opening up open world tracking,” in *CVPR*, 2022. [16](#)
- [288] M. Deitke, D. Schwenk, J. Salvador, L. Weihs, O. Michel, E. VanderBilt, L. Schmidt, K. Ehsani, A. Kembhavi, and A. Farhadi, “Objaverse: A universe of annotated 3d objects,” in *CVPR*, 2023. [16](#)
- [289] Z. Wu, S. Song, A. Khosla, F. Yu, L. Zhang, X. Tang, and J. Xiao, “3d shapenets: A deep representation for volumetric shapes,” in *CVPR*, 2015. [16](#)
- [290] M. A. Uy, Q.-H. Pham, B.-S. Hua, T. Nguyen, and S.-K. Yeung, “Revisiting point cloud classification: A new benchmark dataset and classification model on real-world data,” in *Proceedings of the IEEE/CVF international conference on computer vision*, 2019, pp. 1588–1597. [16](#)
- [291] D. Hegde, J. M. J. Valanarasu, and V. M. Patel, “Clip goes 3d: Leveraging prompt tuning for language grounded 3d recognition,” *arXiv preprint arXiv:2303.11313*, 2023. [16](#)
- [292] A. X. Chang, T. Funkhouser, L. Guibas, P. Hanrahan, Q. Huang, Z. Li, S. Savarese, M. Savva, S. Song, H. Su *et al.*, “Shapenet: An information-rich 3d model repository,” *arXiv preprint arXiv:1512.03012*, 2015. [16](#)
- [293] A. Dai, A. X. Chang, M. Savva, M. Halber, T. Funkhouser, and M. Nießner, “Scannet: Richly-annotated 3d reconstructions of indoor scenes,” in *CVPR*, 2017. [16](#), [17](#)
- [294] H. Caesar, V. Bankiti, A. H. Lang, S. Vora, V. E. Liong, Q. Xu, A. Krishnan, Y. Pan, G. Baldan, and O. Beijbom, “nuscenes: A multimodal dataset for autonomous driving,” in *CVPR*, 2020. [16](#), [17](#)